Masterarbeit
Zur Erlangung des akademischen Grades Master of Science

Thema der Arbeit:
Coupled human physical effects in changing climate: Flood risk management and the levee effect

eingereicht von: Anne Scheibe

Gutachter: Prof. Dr. Tobias Krüger
Gutachterin: Jun.-Prof. Dr. Nicole Glanemann

Eingereicht am Geographischen Institut der Humboldt-Universität zu Berlin am:

Coupled human physical effects in changing climate: Flood risk management and the levee effect

Anne Scheibe[1]

[1]Humboldt University Berlin, Geography Department, Germany; pleseann@hu-berlin.de

Key Points:

- Increasing flood exposure and vulnerability due to flood-protected communities - the levee-effect is observed
- Adaptation measures can not completely mitigate population displacement due to flooding
- Uncertainties in the projections of future developments are significantly higher for the levee-building society vs. levee-less society

Abstract
In 2016, floods accounted for around 50 percent of all climate-related catastrophes worldwide (Munich Re 2016). Temperature increase, sea level rise and storm surges intensify flood risk. Protective measures, such as constructing levees, have been taken to reduce the risk of frequent and coastal flooding. Levees are believed to reduce the exposure and vulnerability of communities to flooding (Di Baldassarre et al. 2015). A movement into the flood prone area results from the construction or elevation of a levee and the population density behind the levee increases. If a flood rises the embankment, the damage can be disastrous (Barendrecht, Viglione, & Blöschl 2017). This false sense of security is called the levee effect.
Hence, this thesis poses the following question: What is the significance of the levee effect related to climate change? Methodically, a research gap is identified and current knowledge from flood risk management is integrated with climate change scenarios into a socio-hydrological model. Therefore the model of Di Baldassarre et al. (2015) was adopted, to capture the levee effect due to climate change. This socio-hydrological model is combined with a time series ensemble of simulated future annual maximal water levels, using the BRICK (Building blocks for Relevant Ice and Climate Knowledge) model (Wong et al. 2017). In addition, sea level rise (SLR) and storm surges were considered under all Representative Concentration Pathway (RCP) Scenarios by using approach of Garner and Keller (2018) and Keller and Srikrishnan (2019, submitted). Thus, the probability of flooding per year until 2100 is determined.

The modeled projections expect an average annual maximum local water level of 3.90 m in 2100, for RCP 8.5 and stationary storm surges, for the tide gauge station Delfzijl (Netherlands). In contrast, this water level increases by 2.50 m (up to 5.60 m) as non-stationary of storm surges are included in the projections. The thesis examines the levee-effect by increasing flood exposure and vulnerability due to flood-protected communities. Additionally, these adaptation measure can not completely mitigate population displacement due to climate change, which is observed as population density decrease by 2100. At the same time, the uncertainties in the projections of future developments are significantly higher for the levee-building society.

This thesis shows considering flood risks from a broad interdisciplinary perspective is helpful and ends with an open discussion on how realistic socio-hydrological models are.

1 Introduction

With losses of around US $320 billion, 2017 was the most expensive year to date worldwide in terms of global weather catastrophes. In the period of 1980 until 2017 the average number of annual natural disasters has increased highly, with hydrological events accounting for the largest part[1]. With every increase of global mean air temperature, the sea level rise (SLR) and the number of storm surges also increase, with the effect of extended global flood exposure (Garner & Keller 2018; Muis, Güneralp, Jongman, Aerts, & Ward 2015; Willner, Levermann, Zhao, & Frieler 2018). In general, climate change has a significant impact on extreme weather events: 65 % of all weather events are influenced by climate change with regard to intensity or frequency (Munich Re 2016). Adaption measures for these risks will become more important over time. Especially political decision-makers need to be able to make significant and future-oriented decisions based on knowledge of the earth's climate system.

The Intergovernmental Panel on Climate Change (IPCC) is the United Nations body responsible for assessing climate change, with scientific input. The IPCC regularly publishes reports based on a review of scientific literature of climate change, its impacts and future risks, as well as on adaptation and mitigation options. The IPCC reports inform governments

[1] https://www.munichre.com/topics-online/en/climate-change-and-natural-disasters/natural-disasters/2017-year-in-figures.html

at all levels and contribute significantly to international negotiations on climate change. In order to explore different future scenarios, four different Representative Concentration Pathways (RCP) were defined and used in climate model simulation. The pathways are RCP 2.6, RCP 4.5, RCP 6.0 and RCP 8.5. They provide different pathways of atmospheric greenhouse gases concentrations. The accumulation of progressive emission of greenhouse gases leads to a warming of global surface temperature, usually defined relative to the pre-industrial reference period 1850 to 1900. With the exception of RCP 2.6, global surface warming is likely to exceed 1.5°C in 2100 in all RCP scenarios. For RCP 6.0 and RCP 8.5 the temperature is likely to increase by more than 2.0°C. In addition, warming will continue beyond the end of the century in all RCP scenarios except RCP 2.6 (Stocker 2014).

The mean global sea level will also rise under all RCP scenarios and is likely to exceed the rate of increase by 2100 over the reference period from 1971 to 2010. Under the RCP 8.5, for example, a global mean sea-level-rise of 0.52 m to 0.98 m by the year 2100 is considered probable (Stocker 2014). Neither temperature changes nor sea-level rise will be spatially homogeneous (Stocker 2014).

It is expected that the impact of floods increase due to population growth, economic development and climate change (Tanoue, Hirabayashi, & Ikeuchi 2016). At the same time, coastal and riverside cities are still attractive trade hubs that have to be protected from the cost-intensive consequences of flooding. Most of all, sea-level rise and storm surges in combination with flooding affects societies that settle in coastal regions, since coastal areas are the most affected regions by increase in extreme weather events. In 2016, for example, a disastrous flood occurred in northeastern France and southern Germany. Tens of thousands of households lacked power, in France the damage was over €1 billion euros and 18 people lost their lives in Germany, France, Romania and Belgium (van Oldenborgh et al. 2016). In 2016, Hurricane Matthew caused losses of $9,700 million in the Caribbean and the USA. In addition, 601 people died as a result of the hurricane. After the devastating consequences for Haiti and the Bahamas, the hurricane hit the coast of Florida and Georgia, where heavy storm surges and offshore winds caused further losses (Munich Re 2016). However, cities along major rivers are also affected by the effects of climate change, partly because precipitation patterns and the resulting floods are changing. For example, several winter storms reached the south of England in 2013/2014, leading to extensive flooding along the Thames River and £451 million of insured losses (Schaller et al. 2016).

In order to reduce the risk of frequent and coastal flooding, protective measures are often taken, by constructing levees. These protective measures are reduce the exposure and vulnerability of societies to floods (Di Baldassarre et al. 2015). Especially through the construction of levees, perceived human safety from floods is increased, because periodic flood events can be prevented (Baldassarre et al. 2013). Accordingly, more people move into the floodplain area and settle relatively close to inundation area. However, if there is a flood-rich period or severe flooding events occur, the damages can be catastrophic (Barendrecht et al. 2017). This so-called "levee effect" results from feedback between the coupled human-flood system, in which the flood awareness of a community has great importance (ib).

1.1 State of the art

After a devastating flood in the southwest of the Netherlands in 1953, the Delta Committee was appointed by the government to develop protective measures against similar future damage caused by flooding (Van Dantzig 1956). This committee asked van Dantzig to estimate the optimal height of levees, by taking an economic decision problem into account, considering the societal costs of investing versus societal benefits of avoiding damage (C. Eijgenraam, Brekelmans, den Hertog, & Roos 2016; Oddo et al. 2017).

According to C. Eijgenraam et al. (2016), this was the starting point of operational research in the Netherlands and the Van Dantzig (1956) case study became a common tool for

flood risk management (C. Eijgenraam et al. 2016; Oddo et al. 2017). Later, C. Eijgenraam et al. (2016) improved the model proposed by Van Dantzig (1956) and developed a levee height optimization model. The results were transferred to all levee rings in the Netherlands and defined a new standard in the Delta Programme 2015 (C. Eijgenraam et al. 2016).

However a modern flood risk management must adapt to the impacts of climate change-related issues. Therefore Garner and Keller (2018) focused their study on uncertainties in sea-level rise and storm surges, which pose considerable risks to coastal communities. In conclusion, they took into account the current impact of climate change on flood events and provided robust statements on adaptive coastal flood defense strategies. Thus, the study of Garner and Keller (2018) is of major importance for this master thesis.

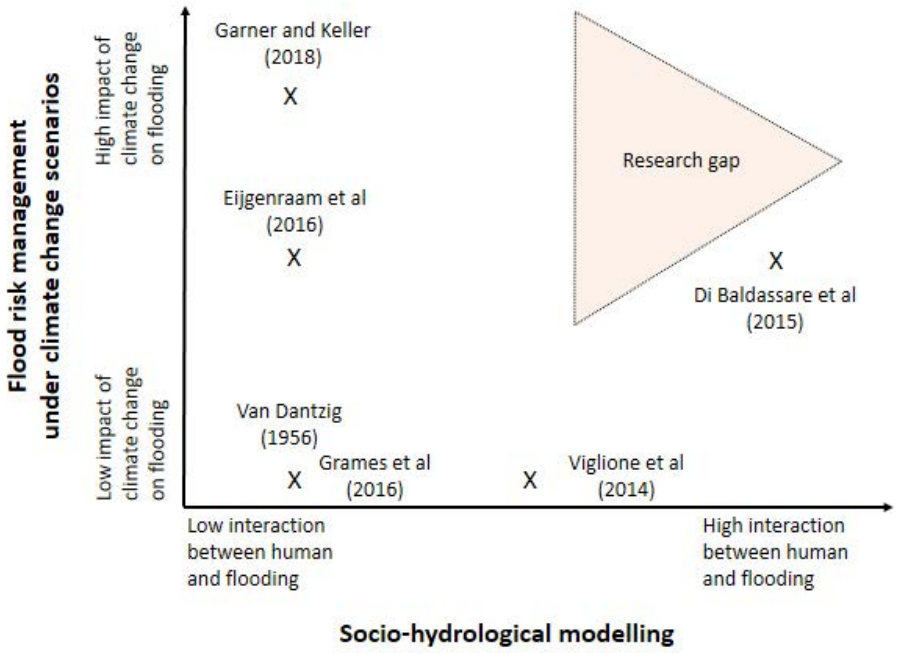

Figure 1: This figure provides an overview about the literature that are of decisive importance for this work and represent the state of the art. The ordinate indicates how intensively flooding has been placed in the context of climate change. The abscissa shows how closely the interaction between humans and flooding is integrated in the relevant studies. Each of the crosses shows the area in which the respective studies can be classified. The research gap is highlighted in a light red triangle.

As shown in figure 1 the flood risk management under climate change scenarios approach is only one part of the research problem. As described before, levees should not be considered in isolation from their environment, but as a coupled system. Therefore also literature dealing with socio-hydrological modelling was reviewed. This type of modeling does not limit physical aspects in the consideration of floods, it also investigates the interaction with humans, whether economic or social. In this way socio-hydrological models contributes to a better understanding of coupled systems (Viglione et al. 2014). Socio-hydrological models can be useful instruments to describe the relationship between a society's vulnerability to a flood event and the expected flood damage. Di Baldassarre et al. (2015) showed that there were two approaches for calculating flood risks. The classical approach is to compare climate change scenarios with socio-economic development, but their study recommends to

improve the traditional approach involving the coupled dynamics of the physical and human system. A representative study for the classical approach in this matter, the work of Grames, Prskawetz, Grass, Viglione, and Blöschl (2016). They developed a descriptive model that characterizes the feedback mechanisms between the community's risk-coping approach, flood damage and economic growth. The bases of their model are the studies from Baldassarre et al. (2013) and Viglione et al. (2014). To determine the effects of the "risk culture" of dynamic communities, Viglione et al. (2014) compared the behavior and coping with flood risks based on three components: collective memory, risk-taking attitude and trust. In the case of flooding, humans realize that their property may be endangered, which in turn leads to the adoption of protective measures against flooding. In this context Viglione et al. (2014) indicate that it is of crucial relevance whether a community itself was affected by a flood and how long ago this event occurred.

Di Baldassarre et al. (2015) use this knowledge and with their socio-hydrology model capture feedback between physical and social processes. In this context they focus on the adaptation and the levee effect. As a result, their study demonstrates that the levee effect becomes apparent in a community building levees for flood protection. Thus, their study also plays a core role in this thesis.

As can be seen from figure 1 and the literature review, there are already a number of studies that prove the relation between increasing flooding and climate change. At the same time, the effects of floods on the social and economic behavior of societies have been investigated. The aim of this thesis is to bring these two approaches together. This leads to the research question: What is the significance of the levee effect in times of climate change? And, is it possible to simulate this effect realistically?

The paper structure is described in the following. The next section contains a short definition of uncertainties. This is intended to put the model output in an appropriate context. It is followed by the methods part, which describes how the water level is sampled and the social behavior is simulated. The model output is presented in the results section and discussed in the subsequent discussion part. A parameter analysis is also performed in this section. In the last part a conclusion is drawn and the results of this thesis are summarized.

1.2 Uncertainties

Models are simplifications of the real world. In complex systems they clarify connections and patterns. Developing a model involves various assumptions and simplifications with respect to the processes being modeled. Simplifications of a complex natural system can be based, for instance, on our current state of knowledge or on the availability of data (Warmink, Janssen, Booij, & Krol 2010). As a consequence, the model output always comes with uncertainties.

Political decisions are based on outputs of climate change related models. Thus, it is necessary that robust statements can be made, especially for policy planning (Hall et al. 2012). In terms of robust decision making, uncertainty is defined as a set of explicit plausible futures that have been chosen to make choices between alternative strategies (Hall et al. 2012). Der Kiureghian and Ditlevsen (2009) argue in their study that these uncertainties can be classified into two possible types, aleatoric and epistemic uncertainties. Aleatoric uncertainty describes the intrinsic probability of a system or model and is also called statistical uncertainty. This uncertainty can change with each new model run (Der Kiureghian & Ditlevsen 2009). Epistemic uncertainty is also termed systemic uncertainty and can be caused by lack of knowledge or lack of data (Der Kiureghian & Ditlevsen 2009). Similarly, Westerberg, Di Baldassarre, Beven, Coxon, and Krueger (2017) propose to distinguish between imperfect knowledge (epistemic uncertainty) and aleatory uncertainties (inherent, stochastic). Thus, in terms of a hundred-year flood event, epistemic uncertainty would be the method of data collection and the natural weather variations would be aleatoric uncertainties (Westerberg et al. 2017). At the same time, it should be noted that the climate system could

suffer abrupt changes in the future, known as tipping points (Lenton et al. 2008), which are difficult to model in any framework.

Decisive for the consideration and categorization of both uncertainties is the present state of scientific knowledge, as well as data availability. Moreover, keeping the complexity of the model at a manageable level is a crucial approach (Der Kiureghian & Ditlevsen 2009), e.g. considering computational complexity. A further source of uncertainty results from the developer of the model itself, because they are limited by their point of view and cultural framework (Wesselink, Kooy, & Warner 2017). At the same time, Westerberg et al. (2017) define further types of uncertainty in relation to flood risk, e.g. the point in time when a flood occurs in the future is an indeterminable uncertainty, as well as social influences resulting from cognitive distortion and heuristics of uncertainties. In addition, being unaware of possible knowledge gaps as a source of model deficiencies (Westerberg et al. 2017).

Uncertainty analysis is recommended in order to be able to estimate the robustness of the model. Hoffman and Hammonds (1994) points out that the aim of the assessment should be clearly defined for the analysis of the model uncertainties (Hoffman & Hammonds 1994). This thesis describes how the levee effect changes under consideration of 4 different RCP scenarios, whereby the use of climate scenarios is already a source of uncertainties related to development of the pathways (Westerberg et al. 2017). Hoffman and Hammonds (1994) recommended a way to determine the uncertainty of model estimation, by producing a set of alternative distributions of parameter values that determine alternative expressions of variability of further risk. This study pursues this approach by considering several possible climate scenarios (RCP 2.6, 4.5, 6.0 and 8.5). In addition, the State of the World (SOW) approach, adopted by Keller and Srikrishnan (2019, submitted), is pursued, which involves the realisation of a unique possible world state per data sample (see section 2.1 below).

Westerberg et al. (2017) present an alternative approach to explicitly and structurally describe the uncertainties of a socio-hydrological system. They propose to design a perceptual model where knowledge about the socio-hydrological system is collected and evolved over time. For this purpose, they publish questions that should be answered in relation to the system in order to develop a better systemic understanding. In addition, this inter- and transdisciplinary approach not only serves to improve one's own understanding, it also furthers consent of stakeholders in terms of flood risk uncertainty. It is expected that this type of uncertainty assessment will contribute to prioritising research efforts and developing a better understanding of the importance of uncertainty (Westerberg et al. 2017). The perceptual model can be designed in three steps of identification and assessments: first, uncertainties and problems in the system, second, sources of uncertainties in the socio-hydrological system and third, classification of interactions in uncertainties (Westerberg et al. 2017).

The following section describes how the model of this study is developed.

2 Methods

This section describes how the model is structured. The first part of the model, the sampling of the water level projection, was adopted from Garner and Keller (2018), a detailed description can be found in their work. The second part of the model is based on Di Baldassarre et al. (2015).

2.1 Water level projection

The water level input data for the model runs are provided by BRICK (Building blocks for Relevant Ice and Climate Knowledge, (Bakker, Wong, Ruckert, & Keller 2017)) v0.2, which is a basic model framework for estimating global mean temperature and regional sea-level. The hindcast-enabled model is used to identify coastal flood regions of risk (Bakker et

al. 2017; Wong et al. 2017). The surface temperature rises due to the amount of accumulated carbon emission in the atmosphere. To project different pathways the simulations are carried out for the four different RCPs 2.6, 4.5, 6.0 and 8.5. The projected increase in global mean surface temperature influences the global sea-level rise. BRICK includes a regional sea-level rise module that translates the global mean sea-level contributions to the regional sea-level at a user-defined location (Wong et al. 2017).
For this study, 13,276 simulation for each RCP scenario were used from BRICKS, providing annual global sea-level projections. These sea-level projections were transformed to absolute local mean sea-level projection at the Delfzijl tide gauge station (Netherlands) for the years 1850 to 2100. As this thesis considers future impacts of climate change, the local sea-level have been normalized to the year 2017.

Under climate change and rising sea levels it is very likely that storm surges will intensify and become more frequent (Keller & Srikrishnan 2019, submitted). To take this effect into account, the storm surges are added to the simulated local sea-levels. In this thesis, it is differentiated whether the storm surges are considered as stationary events, i.e. do not intensify while temperature rises, or whether they are non-stationary and intensify with the temperature rise. Storm surges are extreme hydrological events. The Generalized Extreme Value-distribution (GEV) is used to estimate the entire spectrum of these occurrences. In general, the GEV is commonly used in the context of extreme value analysis and incorporates Gumbel-, Frechet- and Weibull-distributions (Martins & Stedinger 2000). The GEV-distribution is defined by its location, scale and shape (Schönwiese 2013). Keller and Srikrishnan (2019, submitted) use a GEV-distribution to take the stationarity of storm surges into account, adding them to the local mean SLR. The GEV distributions were estimated for stationary and non-stationary storm surges. Both cases were calculated using Markov Chain Monte Carlo simulation and data from the Delfzijl tide gauge station. A state of the World (SOW) approach was pursued, which includes the realization of a unique state of the world per data sample (Keller & Srikrishnan 2019, submitted). Finally, annual maximum sea level series are generated by combining a local relative mean sea level based on the GEV-distribution (Keller & Srikrishnan 2019, submitted). An ensemble of 10,000 SOWs was used to represent the sea-level rise and the storm surge distribution. These annual maximum sea level series are implemented into the model of this study as water level W.

2.2 Social behavior projection

The model of this thesis and the formulas below are adopted from Di Baldassarre et al. (2015), who implemented two types of societies. A society that built levees to protect itself against floods (levee-building society, "techno society" in Di Baldassarre et al. (2015)) and a society that does not build levees (levee-less society, "green society" in Di Baldassarre et al. (2015)). A basic assumption of the model is that humans, depicted as population density D, settle near to a flood prone area. In case of flooding the community has two possible reactions. On the one hand the community is shocked and builds a memory, expressed by social memory of floods M, and moves out of the flood prone area, reducing its population density. This is equivalent to moving out of the flood prone area. On the other hand, the community builds a levee or elevates an exiting one, expressed as the height of levees H, which protects against further floods.

Flood and community interactions are defined as:

$$\frac{dD}{dt} = \rho_D \ (1 - D_t(1 + \alpha_D \ M_t)) - L_t \tag{1a}$$

$$\frac{dH}{dt} = P_t - \kappa_T \ H_t, \tag{1b}$$

$$\frac{dM}{dt} = L_t - \mu_s \ M_t. \tag{1c}$$

Equation (1a) depicts the dynamic of population density including the constants ρ_D (maximum relative growth rate) and α_D (expression of preparation for and awareness of a flood event). Furthermore, the variables social memory and loss are included in the calculation of population density.

Subsequently, the loss L is subtracted and defined as follows:

$$L_t = F_t \cdot D_t. \tag{2}$$

The loss results from flood damage and population density. Thus, with higher loss, population density will be lower (1a).

The second dynamic equation (1b) defines the height of the levee. The levee height is calculated by a decay rate κ_T and the protection level P. Only the levee-building society prevents flood damage by elevating levees. This enhancement of protection level is defined as

$$P_t = \varepsilon_T(W_t + \xi_H H_t), \tag{3}$$

where ε_T is a safety factor for the levee elevation. This implies that the levee is constructed a bit higher than the previous water level, which had exceeded the embankment.

The third equation (1c) describes the dynamic of community's memory effected by flooding. The social memory is calculated by the memory loss rate (μ_s) and the community's loss. Hence, a high amount of loss increases social memory influenced by flooding.

In any case, a relative flood damage F occurs to the communities and is defined as:

$$F_t = 1 - \exp\Big(-\frac{W_t + \xi_H H_t}{\alpha_H}\Big) \quad \text{if} \quad W_t + \xi_H H_t > H_t. \tag{4}$$

Flood damage occurs when the water level (see section 2.1) crosses the embankment ($W_t + \xi_H H_t > H_t$). Here ξ_H is a constant that is multiplied by the levee height, since it is assumed that the presence of a levee already elevates the natural water level. The parameter α_H is corresponding to the ratio between flood levels and relative damage. There is no damage to the levee-building society in the presence of a levee when the levee is higher than the current water level. Thus, the community is protected from flooding by its adaptation measures. The levee-less society suffers damages at every water level.

Table 1 in the supplement provides the parameters used in the simulations. The corresponding initial values for equations (1) and equations (4) are listed in table 2 in the supplement.

3 Results

In this section the research results obtained during the model run for 10.000 SOWs are summarized.

3.1 Water level projection

The sampled data starts in 1850. The main focus of this work is on the future of climate change, for this reason the historical time series was calibrated and no water levels above 5 m were considered (see section 4).

Figure 2 depicts the water level projection for the RCP scenarios 2.6 and 8.5 as well as stationary and non-stationary storm surges (results for all RCP scenarios are provided in figure 6).

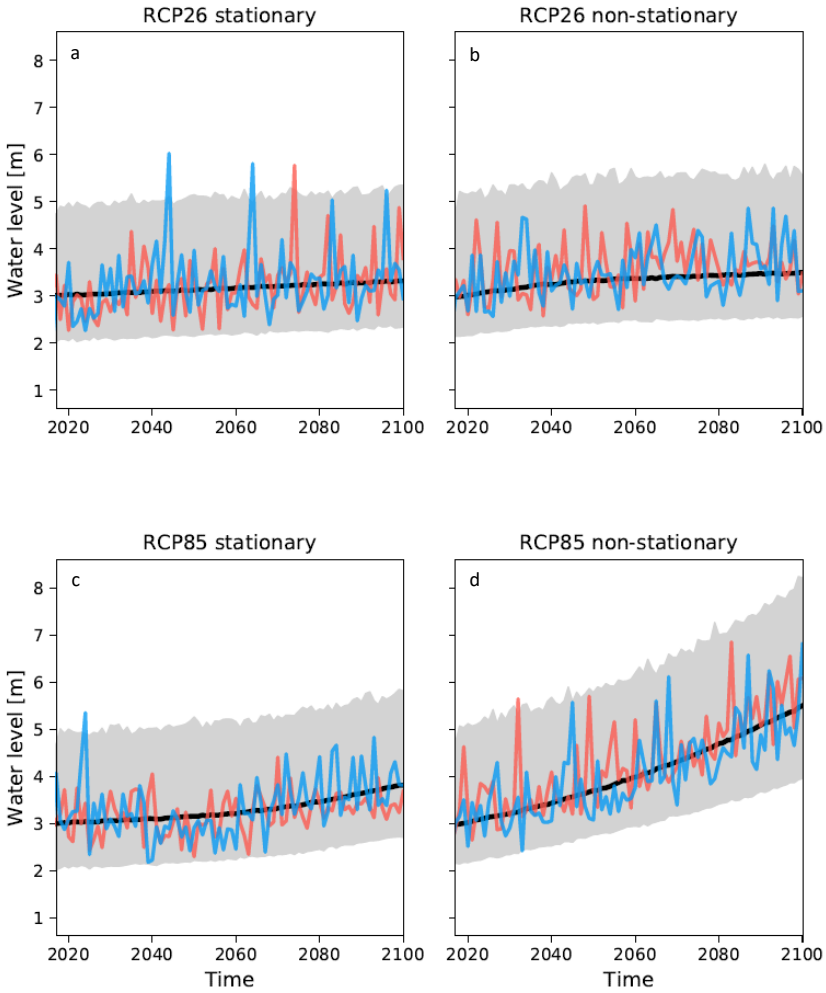

Figure 2: The figure shows the relative distribution of frequencies in relation to the expected water level from 2017 onward. The grey bar indicates the 99.5% quantile at the upper limit and the 0.5% quantile at the lower limit, per year. The black line represents the median of the sample distribution. The red and blue lines are two time series from the data sample as illustrative examples. This analysis was made for the RCP scenarios 2.6 (a,b) and 8.5 (c,d), as well as for stationary (left) and non-stationary (right) of storm surges.

As mentioned in section 2.1, the water level corresponds to the maximum local water level of the tide gauge station Delfzijl (Netherlands). Figure 2 summarizes the relative distribution of frequencies with respect to the expected water level from 2017 onward. For the expected maximum and minimum annual water level, the 99.5% quantile and the 0.5% quantile were regarded as upper and lower limits of the frequency distribution. The range of both quantiles can be seen in the gray bars in the figure. The black line shows the median of the sampled distribution. The red and blue lines correspond to two different time series of

the data sample and illustrate how the time series are shaped. According to figure 2 , the water level for RCP 2.6 has its distribution for the median of frequencies at about 2.9 m (standard deviation, $\sigma = 0.2$ m) for stationary and 2.7 m ($\sigma = 0.5$ m) for non-stationary. The water level for RCP 8.5 has its distribution for the median at about 3 m ($\sigma = 0.3$ m stationary, $\sigma = 0.9$ m non-stationary).

The trend of the median and the table 3 in the supplement show that the annual maximum sea level at the tide gauge station in Delfzijl increases from 2017 to 2100 by 0.30 m under stationary and 0.50 m under non-stationary storm surges under consideration of a moderate climate scenario (RCP 2.6). Under RCP 8.5, the water level is projected to increase from 2017 to 2100 by 0.80 m under stationary storm surges and by 2.50 m under non-stationary storm surges.

3.2 Social behavior projection

In figure 3 and 4 the temporal evolution of the levee height (a-b), the social memory (c-d), the population density (e-f) and the losses (g-h) for the RCP scenario 8.5, under consideration of stationary as well as non-stationary storm surges is shown. The panels of figure 3 show the projections for the levee-building society and in figure 4 for the levee-less society.

The **levee height** is only meaningful for the levee-building society (in figure 3(a-b)). It can be seen that the range between the 0.5%- and 99.5%-quantiles at the end of the century is gaining in width, this increases with non-stationary storm surges. Therefore, under the RCP scenario 8.5 the levee at the tide gauge station Delfzijl is 5.70 m high in 2017 and 6.40 m high in 2100 during stationary storm surges. Considering non-stationary storm surges, the levee height in 2017 is 5.41 m and 8.10 m at the end of the century. The median of the data distribution is on an average of 5.07 m ($\sigma = 0.84$ m) for stationary and 5.22 m ($\sigma = 1.10$ m) for non-stationary storm surges. The two example time series, marked with a red and a blue line, show that under non-stationary storm surges up to 2100, flooding occurs more frequently, crossing the embankments.

That is also reflected in the figure of the **social memory** of the levee-building society (c-d). The levees provide protection to the community for a certain period of time. As the period of protection increases and society does not suffer from flooding, its memory of the event fades away and social memory decreases. However, the course of the median shows that the social memory rises until the end of the century. Thus the social memory is 0.06 in 2017 for stationary storm surges and 0.14 in 2100. Under consideration of non-stationary storm surges, the social memory is 0.10 in 2017 and 0.24 in 2100.
The figures of the social memory differ visibly between the two types of society. The social memory of the levee-less society in figure 4 (c-d) has a constant slightly increasing trend, with a median of 0.35 ($\sigma = 0.06$ m stationary, $\sigma = 0.07$ m non-stationary) and is well above the average of the levee-building society, because these are not protected against flooding. Thus they suffer frequent floods and their social memory does not decrease and rises slightly towards the end of the century.

The **population density** of the levee-building society is shown in the figure 3 (e-f) and that of the levee-less society in the figure 4 (e-f). The course of the population density of both communities is contrary to the course of the social memory. As can be seen in figure 3 (e-f), the median of the distribution decreases significantly until the end of the century. In 2017 the population density is 0.72 and in 2100 0.53, assuming stationary storm surges. Considering non-stationary storm surges, the population density is 0.62 in 2017 and 0.27 in 2100. This strong reduction in population density since 2080 is also reflected in the reduction of the grey errorbar. Levees are a possible adaptation measure, but they can not completely mitigate the emigration due to climate change. Similarly, the levee-less society reduces its population density by 2100, but more moderately than the levee-building society. Assuming stationary storm surges, their population density is 0.09 in 2017 and 0.07 in 2100. Taking

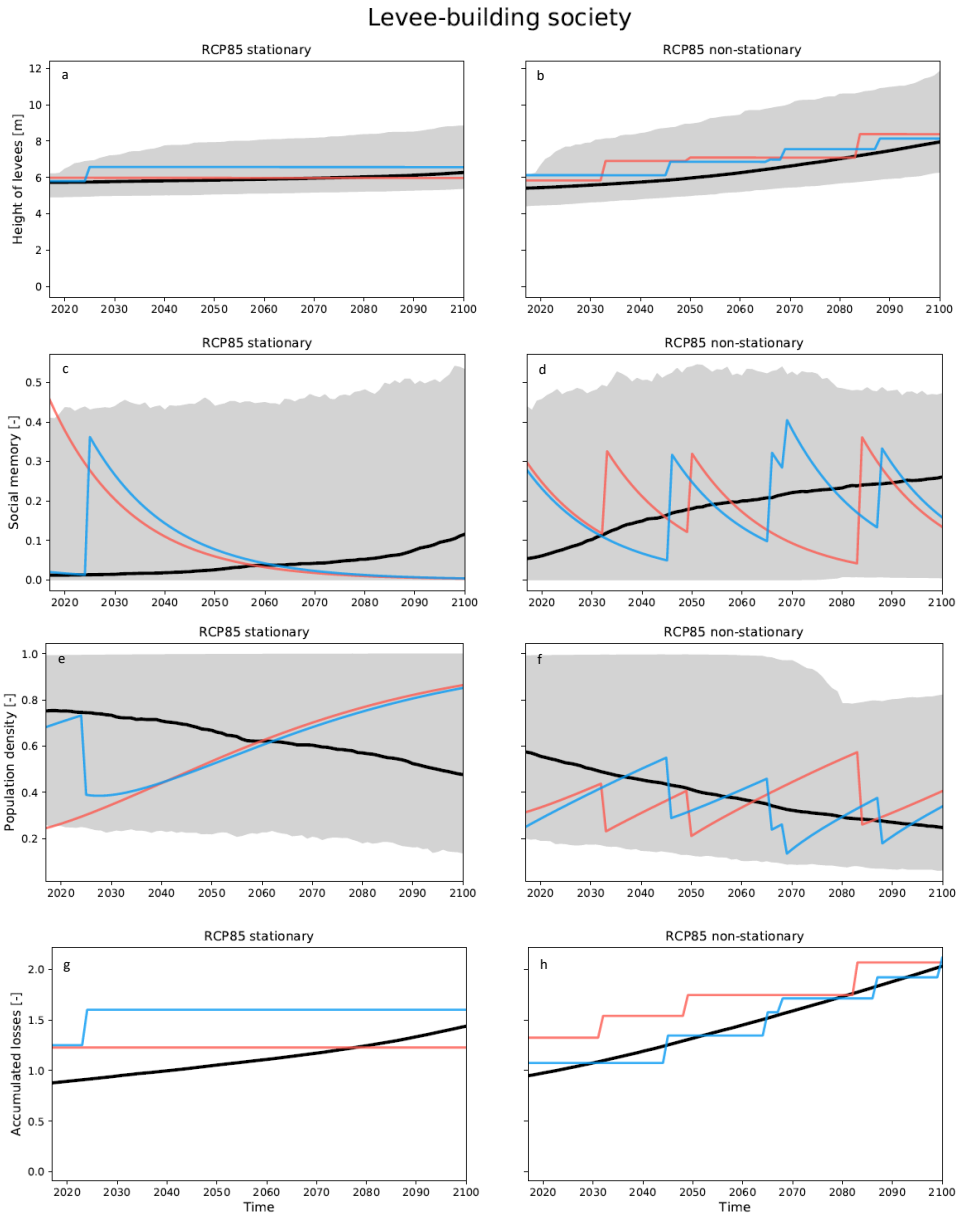

Figure 3: The panels show the projections for the levee-building society. The variables levee height (a-b), social memory (c-d), population density (e-f) and accumulated losses (g-f) for the RCP scenario 8.5, under consideration of stationary (left) and non-stationary (right) storm surges are depicted. For the expected maximum and minimum values of the distribution, the 99.5% quantile and the 0.5% quantile were regarded as upper and lower limits. The range of both quantiles can be seen in the gray bars in this figure. The black lines show the median of the projected distributions. The red and blue lines correspond to two different time series of the projected data and illustrate how the time series are shaped. Here, a temporal resolution with annual time steps from 2017 to 2100 is shown.

non-stationary storm surges into account, the population density is 0.09 in 2017 and 0.06 in 2100.

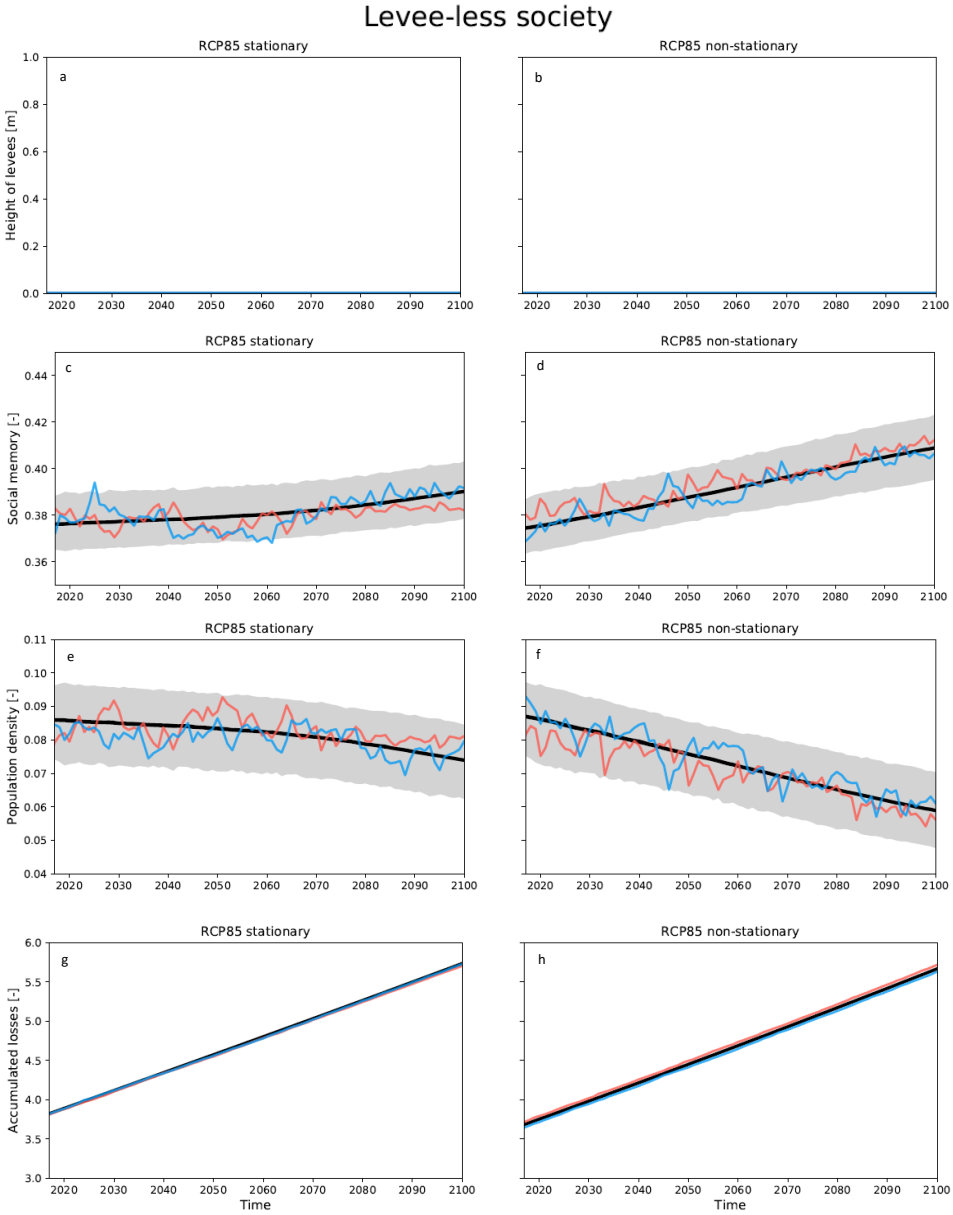

Figure 4: The panels show the projections for the levee-less society. The variables levee height (a-b), social memory (c-d), population density (e-f) and accumulated losses (g-f) for the RCP scenario 8.5, under consideration of stationary (left) and non-stationary (right) storm surges are depicted. For the expected maximum and minimum values of the distribution, the 99.5% quantile and the 0.5% quantile were regarded as upper and lower limits. The range of both quantiles can be seen in the gray bars in this figure. The black lines show the median of the projected distributions. The red and blue lines correspond to two different time series of the projected data and illustrate how the time series are shaped. Here, a temporal resolution with annual time steps from 2017 to 2100 is shown.

The accumulated **losses** for both types of society are depicted in figure 3 (g-h) and 4 (g-h). The figures show the accumulated loss over time. The levee-building society has

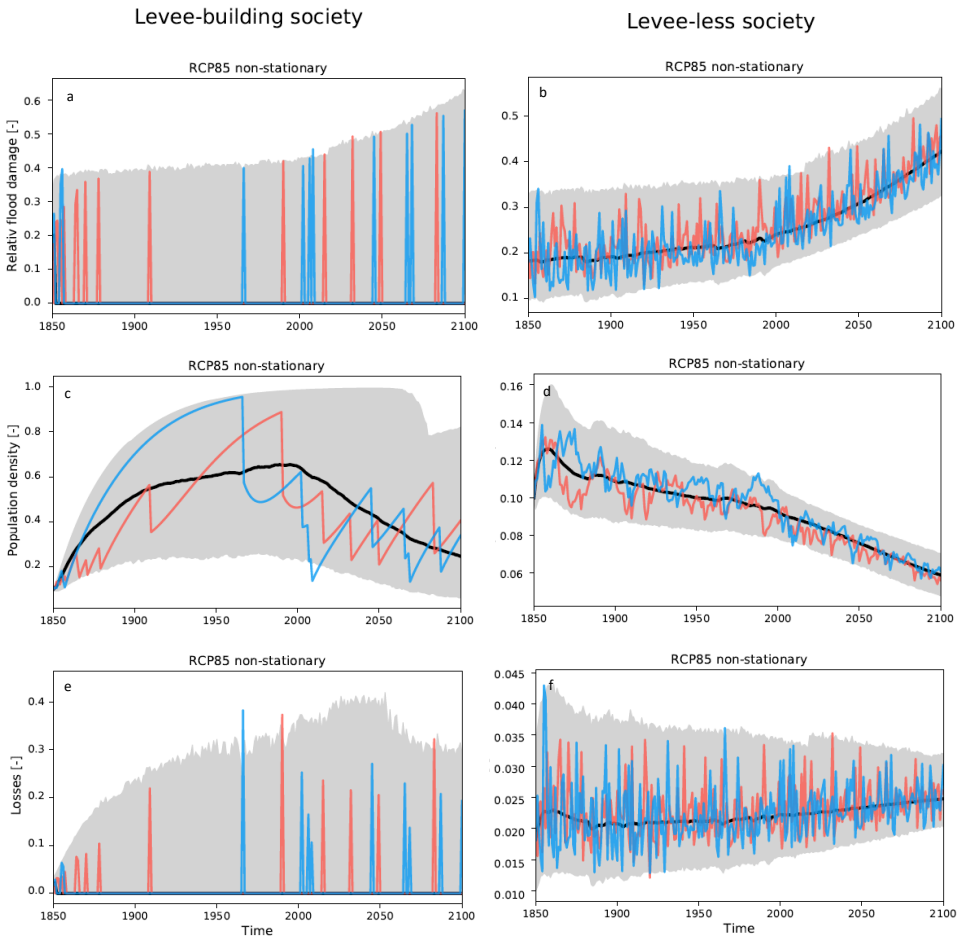

Figure 5: Levee effect. The variables flood damage (a-b), population density (c-d) and loss (e-f) for the RCP scenario 8.5, under consideration of non-stationary storm surges are depicted. The levee-bulding society is shown on the left side and the levee-less society on the right side. For the expected maximum and minimum values of the distribution, the 99.5% quantile and the 0.5% quantile were regarded as upper and lower limits. The range of both quantiles can be seen in the gray bars in this figure. The black lines show the median of the projected distributions. The red and blue lines correspond to two different time series of the projected data and illustrate how the time series are shaped. Here, a temporal resolution with annual time steps from 2017 to 2100 is shown. Here, a temporal resolution with annual time steps from 1850 to 2100 is shown.

a accumulated loss of 0.9 in 2017 and of 1.4 in 2100, considering stationary storm surges. Assuming non-stationary storm surges, their accumulated losses is 1.0 in 2017 and 2.0 in 2100. The red and blue lines show that losses occur at certain points in time and the level of loss continues until a flood crosses the embankment. The accumulated losses of the levee-less society are significantly higher than those of the levee-building society, however they increase as well until 2100. This is reflected by the fact that the accumulated loss is 3.82 in 2017 and 5.73 in 2010, taking stationary storm surges into account. Considering non-stationary storm surges, the loss is 3.68 in 2017 and 5.67 in 2100. The two example time series in red and blue lines are close to the mean, indicating continuous flood loss in this type of society.

This continuous flood losses suggest that the levee-less society is facing a higher **flood risk**. According to Kron (2005), flood risk is calculated by hazard, exposure and vulnerability. Transferred to this model the variable water level can be associated as hazard. For the levee-less society, any water level will cause damage, and for the levee-building society damage occurs only if the water level crosses the embankment. The vulnerability is directly affecting the variable population density, because the society reacts with a direct reduction of population density in case of a flooding. Flood exposure refers to the variable levee height. In case of the levee-less society, exposure is constant over time. The flood exposure of the levee-building society increases over time, due to the construction of levees and the associated **levee-effect**.

An interpretation of this reflection can be given by figure 5 were the variables expressing flood risk are depicted. As argued before, the accumulated losses of the levee-less society are higher than those of the levee-building society, but that is due to the fact that the levee-less society are subject to annual losses (see figure 5 (f)). In contrast, the maximum expected losses of the levee-building society are significantly higher (see figure5 (e)). This suggests that the levee-building society is subjected to immediate very high damage in certain points of time, allowing conclusions regarding the levee effect. In general, the flood damage between the two types of society is approximately equal (compare panels of figure 5 (a-b)), but more people live in the community with adaptation measures (compare panels of 5 (c-d)). As the losses arise from flood damages and population density, the losses within the levee-building society are always higher than those of the levee-less society. Which also expresses a characteristic of the levee effect.

In general, the results of the projections indicate population displacement of inhabitants will increase until the end of the century, regardless of whether society protects itself with levees or not. The uncertainties in the consideration of future developments are significantly higher for the levee-building society. In addition, it can be seen that the differentiated observation of storm surges is justified. Assuming non-stationary storm surges, there will be more frequent events by the end of the century than under consideration of stationary storm surges. As a result, the probability of flooding, passing over embankments and causing damage increases. In addition, the standard deviations for the forecasts due to non-stationary storm surges are higher - hence, there is a higher uncertainty in the projection.

As described by Di Baldassarre et al. (2015) and Barendrecht et al. (2017), the model outputs also show that more people live in flood-protected communities, leading to increased flood exposure and vulnerability.

4 Discussion

This section aims to contextualize the projections of this work in a literature review. At the beginning a parameter analysis is presented, which was carried out for the parameters floodwater vulnerability (α_H) and memory loss rate (μ_s). Subsequently, it is discussed whether the integration of economic aspects into the choice of flood risk management instruments could be useful. Finally, it is discussed how realistic the results of this work are and how far modeling is realistic.

4.1 Parameter analysis for floodwater vulnerability (α_H) and memory loss rate (μ_s)

The following parameter analysis is aimed to determine the influence of the parameters floodwater vulnerability (α_H) and memory loss rate (μ_s) on the modeled variables. The interpretation of the results (section 3) shows that the social memory has a great impact on the variables population density and loss. At the same time, as can be seen in equation 1, the social memory is mainly determined by the constant parameter memory loss rate. Therefore this parameter is investigated more closely. The second parameter to be considered is the

floodwater vulnerability. This parameter was adopted from Di Baldassarre et al. (2015) and appears to be very high with a value of 10 m.

From a purely mathematical point of view, it makes sense to express the flood damage (equation 4) as an exposure function. Within this function the parameter floodwater vulnerability causes that not every damage is fully included in the calculation, but exponentially, up to a height of $\alpha_H = 10$. Only if a water level of 10 m is reached, the damage is fully reflected in the calculation.

The parameters floodwater vulnerability and memory loss rate are varied with the following values:
μ_s = 0.015, 0.03, 0.06, 0.12, 0.24 (Di Baldassarre et al. 2015) and
α_H = 4.5 (Keller & Srikrishnan 2019, submitted), 5, 6, 7, 8, 9, 10, 12, 15.

The parameter analyses for floodwater vulnerability and memory loss rate is using the maximum value of the 99.5%-quantile of the distribution of output variables (according to RCPs and storm surges). The results are shown in the supplement (see 20, 21, 24, 25) and discussed as follows.

Social memory (M)
A decrease in floodwater vulnerability and memory loss rate causes an increase of social memory. When the floodwater vulnerability parameter is low, the damages caused by flooding are higher. At the same time, the social memory rises with each flood event, which then only declines over time. Heatmap 20 for the levee-building society shows that the influence of the memory loss rate on the social memory is more significant than the level floodwater vulnerability. These impacts can be seen even more clearly for the levee-less society (see figure 21).

Population density (D)
As social memory increases, population density decreases and vice versa. Immediately after a flood event occurs there is a movement away from the flood prone area. With decreasing memory of the event, the population density rises again. Figure 22 shows that the memory loss rate has a significant impact on population density. Only with a very low memory loss rate ($\mu_s = 0.015$) can small differences be observed with regard to floodwater vulnerability. A low floodwater vulnerability leads to a low population density.

In conclusion, it can be argued that the attractivity of the flood prone area for the levee-building society increases when the floodwater vulnerability parameter is high. This effect is also most evident for the levee-less society (see figure 23), that means the higher the floodwater vulnerability value, the higher the population density.

Concerning, because floodwater vulnerability is a parameter associated to the relationship between flood water levels and relative damage.

For the reason that the levee-less society is unprotected against flooding, the amount of this parameter is relevant, because the higher it is assumed, the lower the damage will be (see equation 4). At the same time the memory loss rate has no significant impact on the population density of this society.

Losses (L)
Losses of the levee-building society are at their highest when floodwater vulnerability is low ($\alpha_H = 4.5$ m) and memory loss rate is high ($\mu_s = 0.24$). For the reason that the floodwater vulnerability is low, damage occurs even at a lower flood water level. Accordingly, more damage occurs at the same water level. If memory loss rate is high,the social memory will decrease and at the same time more people move into the flood prone area again, increasing the population density. Since the losses of a society are calculated from the product of population density and flood damage (see equation 2), the loss increases as well. Compared to the levee-building society, the loss of this community type is low. The damage is again

highest when floodwater vulnerability is lowest. For the lowest floodwater vulnerability (α_H = 4.5 m) the loss is 0.06. This value is constant over all variations of the memory loss rate, which allows the conclusion that the loss of the levee-less society is mainly determined by floodwater vulnerability. Only at a level of α_H = 10 m, there are minor changes in the loss corresponding to the memory loss rate.

In summary, the parameter analysis confirms the coherence of the model. The variables levee height, social memory and population density depend on each other. A model run with a floodwater vulnerability of α_H = 4.5 m and a memory loss rate of μ_s = 0.06 shows that the decrease of the parameter compared to the original model run causes the damage to increase. There are no unexpected dynamics in the model.

4.2 Socioeconomic interpretation

In this context, it should be noted that the model of this study does not follow an economic approach. The integration of cost-benefit decisions could enable a more realistic focus. Deciding whether and to what extent measures should be implemented to protect against flooding represents is a complex process.

Simply constructing or elevating levees and moving away would not be a practical approach as the only flood coping strategy. Large cities are still located along rivers or at ports due to facilitating trade. They are attractive locations for both employees and businesses. Moving out of the flood prone area following a flood, as in the model of this study, wouldn't be a practical solution. The damage incurred would be considered and the measures to be taken to avoid or minimise further damage would be assessed. Several flood risk protection options would be considered. Politically, it is an important decision how much financial support is given and which measures should be taken for flood risk management. C. Eijgenraam, Brekelmans, den Hertog, and Roos (2012) determined the safety standards for the levees in the Netherlands, using a cost-benefit analysis. The estimations derived from their optimization model were applied to all levee rings in the Netherlands and defined as standards by the government.

One more broad approach to support political decision-making is to include Shared Socioeconomic Pathways (SSPs) to consider possible pathway of economic development and population growth. The four different RCPs with their levels of greenhouse gases emissions do not contain a socio-economic "narrative". Societal decisions and actions which have an impact on greenhouse gas emissions, are considered in the SSPs. The SSPs are a scenario framework combining the RCPs in a scenario matrix architecture (Riahi et al. 2017). The RCPs define which greenhouse gas concentration will lead to different levels of warming and the SSPs point out which conditions have an influence on emissions. The SSPs have been developed by the climate change research community and they integrate analysis of future climate impacts, vulnerabilities, adaptation and mitigation (Riahi et al. 2017). Five different narratives describe various states of the world. These different baseline worlds contain different factors, such as population density, economic growth (GDP), urbanization and technology, which lead to very different future emissions and warming patterns.

One main application is on policy and cooperation which will determine how the Paris Agreement goals can be reached [2].
Described by ONeill et al. (2014) and Riahi et al. (2017) the different narratives are characterized as follows: SSP1 is called "Sustainability - On the Green Path" and there are low challenges to mitigation and adaptation. Perceived environmental boundaries are respected. Demographic change is accelerated by investment in education and health. Economic growth is shifting towards a focus on human well-being. SSP2 is the "Middle of the Road" scenario with medium challenges in mitigation and adaptation. Social, economic and technological

[2] https://unfccc.int/sites/default/files/part1_iiasa_rogelj_ssp_poster.pdf

trends are essentially based on historical patterns. This scenario is an intermediate pathway between SSP1 and SSP3. SSP3, the "Regional Rivalry - A Rocky Road", is describing high challenges in mitigation and adaptation. There is a focus on national or regional issues. Countries focus on their own protection, such as security, energy and food, and investment in education and technological development is declining. Economic development is slowing down and population growth is decreasing in industrialized and increasing in developing countries. Environmental concerns receive little international priority. SSP4 is called "Inequality - A Road Shared" and projects low challenges to mitigation, but high challenges to adaptation. Increasingly unequal investment in human capital, differences in economic opportunities and political power relations lead to disparities between and within individual countries. Relatively rapid technological developments are contrasted with high inequalities in national economies. SSP5 is titled "Fossil fired development - On the highway", describing high challenges to mitigation and low challenges to adaptation. High investments in human and social capital, increasing market competitiveness, innovation and technological progress lead to rapid economic growth. The world population will peak at the end of the century.

Taking population density and GDP per capita into account is clearly important for flood risk modeling. According to Jongman, Ward, and Aerts (2012), the total flood risk rises from 46 trillion USD in 2010 to 158 trillion USD in 2050, additionally the total flood exposure of 27 trillion USD in 2010 increase to 80 trillion USD in 2050 (land-use based assessment). Assuming a SSP5 pathway for the model of this study, it could result that a strong economic development leads to high damages in case of a flooding. At the same time a high level of innovation potential is considered in this pathway and rapid developments in adaptation measures could happen as well, reducing damages, for example, by intelligent levees[3]. C. J. Eijgenraam (2006) raises the question of whether future developments in technical progress can reduce the investment costs for elevating levees. In other words, it would be interesting to see what the future projections would look like under assumption of the SSP5 scenario.

Another possibility to integrate the SSPs into the model of this study would be to consider population density projections. In all case of the modeled outputs of this thesis, the population density decreases until the end of the century. However, since the SSP-scenarios project a increase in the world population at lest until the 2050ies. Therefore, the trend or the development of the population density could be considered in the model of this study.

In general, it appears that the global economic damage caused by floods will increase faster than global economic prosperity (Winsemius et al. 2016). Rising global economic burdens due to flood damage require adaptations. Both high and low income countries can benefit from investments in adaptation measures (Winsemius et al. 2016), as the risk of flooding is reduced due to investments in flood protection (Jongman et al. 2014).

The implementation of economic developments and population growth in the socio-hydrological model of this thesis suggests a meaningful extension that could lead to new insights.

4.3 Conceptual modeling and realism

Modeling human-water interaction is a complex problem. Wesselink et al. (2017) conducted a literature review to find out how water has been conceptualized in natural and social science so far. They argue that it would be beneficial to make use of the plurality that is needed from the topic and to work on it in an interdisciplinary way. In general, it seems to be a good approach to consider historical flood events and behavior patterns and to use them as a narrative for a model. The role of the human being within the human-water-interaction

[3] In the future, levees will be more robust, multifunctional and fracture-resistant `http://dutchdikes.net/future/`.

should be expanded considerably more. However, this is not simple, since human behavior can be very individual and shaped by norms and values. One possible approach to take this into account is agent-based modeling (Wesselink et al. 2017).

In contrast to that, Massuel et al. (2018) did empirical studies in North Africa researching co-evolution of society and water. Thereby they consider humans and their activity as part of the water cycle and not just as boundary conditions within a socio-hydrological model. For many scientific models consistency is assumed which cannot be transferred to human way of behavior. In sociology basic laws, as in physics or biology, do not exist. Although conclusions about human behavior can be drawn from historical data, they are not indicators of future behaviour, as not all determinants are known (Massuel et al. 2018). In addition, Massuel et al. (2018) point out that there is a difference in how dynamics are defined in natural and social sciences. It is a quantitative component in the natural sciences, but not in sociology. This can lead to misunderstandings about epistemological concepts (Massuel et al. 2018).

Di Baldassarre et al. (2015) developed a model suitable for reproducing the interactions between flood events and humans (Wesselink et al. 2017). The difference to the model of this study is that Di Baldassarre et al. (2015) have used artificial time series as input variables, whereas climate model data are used in this study.

In this study, the estimated output for RCP 8.5, considering non-stationary storm surges, shows that levees will have an height of 8.10 m by the end of the century. Compared to 2017 (5.41 m), levees will be elevated by 2.70 m. But the range of the grey errorbar in figure 3 for the height of levees (b) show that they could potentially be built higher. They might be elevated up to 9.07 m ($\sigma = 4.31$ m; 99,5%-quantile value at 2010). This elevation rate is similar to the projections of C. Eijgenraam et al. (2012) and their optimization model. They point out that several levee rings in the Netherlands should be elevated between 2.60 m and 3.63 m during the next 75 years (C. Eijgenraam et al. 2012). In comparison, the projections of Di Baldassarre et al. (2015) modeled levee height to go up to 20 m until the end of this century (Di Baldassarre et al. 2015).
For first model runs of this thesis, the water level were not historically constrained for the time period between 1850 and 2017. As a result, under RCP scenario 8.5 the levees would already have been more than 15 m high before 1900 (see figure 19). Including non-stationary storm surges, the levees would have been built over 35 m high until 2100. This is quite unrealistic, because in order to avoid construction breakdowns, levees must have a certain level of protection or otherwise they would collapse long before the water would pass over the embankment (C. J. Eijgenraam 2006). For example, such a levee break occurred during Hurricane Katrina in August 2005 in the city of New Orleans (USA). The major part of flooding in New Orleans was not caused by an overtop of embankments, it was due to human error in the planning and construction of the levees[4].

If a levee is intended to be built high, it will have to expand widely to withstand the pressure of water and provide sufficient infiltration space. Figure 18 shows that the elevation of a levee is in strong conflict with land use. A levee that is only 2 m above NAP (Amsterdam Ordnance Date or Normaal Amsterdams Peil) needs a width of about 35 m (Zeeberg 2009). In order to achieve a more realistic output, the model input of this thesis is pre-selected. The historical data (1850-2017) of the annual maximum water level was limited to have a maximum height of 5 m. This height corresponds to the levels that levees in the Netherlands currently have, about 4.5 (Zeeberg 2009). Keller and Srikrishnan (2019, submitted) uses this

[4] `https://www.nature.com/news/2005/051031/full/news051031-9.html`

value as an initial levee height too. However, as floods occurred in the Netherlands during this period [5], the maximum water level in this study is set slightly higher ($\leqq$ 5 m).

In summary, the implication of SSPs and a validation with historic data could be a possible avenues for further research.

5 Conclusion

The projections of this study indicate that the annual maximum local water level is likely to increase by the end of the century. It makes a significant difference whether considering a moderate climate change scenario such as RCP 2.6 or a business as usual scenario such as RCP 8.5. Furthermore, the assumption that storm surges will intensify with the rise in global mean surface temperature becomes relevant. Assuming that storm surges are non-stationary, the increase of the predicted maximum local water level intensifies drastically. The tide gauge station Delfzijl (Netherlands) can expect an average annual maximum local water level of 3.90 m in 2100, for RCP 8.5 and stationary storm surges. In contrast, this water level increases by 2.50 m (up to 5.60 m) as non-stationary of storm surges are included in the projections (see table 3). As a result of the increase in the water level, the protection measures of the levee-building society were developed further. Therefore, the levee at the Delfzijl tidal station is about 5.41 m in 2017 and 8.10 m at the end of the century, taking RCP scenario 8.5 and non stationary of storm surges into account. As can be seen in figure 16 in the supplement, the frequency of flood events crossing the embankment is more often when considering non-stationary of storm surges.

Levees are a possible adaptation measure against flooding, but they can not completely mitigate forcing people to move due to climate change. Considering non-stationary storm surges, the population density of the levee-building society is 0.62 in 2017 and 0.27 in 2100. A significant decline in population density beginning in 2080 is reflected in figure 3 (f). Additionally, even if the levee-less society expects periodic flooding, they reduce population density by 2100 too. Therefore, both societies exhibit an increasing vulnerability towards the end of the century by population density decline.

In total, the population density of the levee-building society is considerably higher than that of the levee-less society. This suggests that people feel more safely behind a levee. The losses, of this study, arise from flood damages and population density. In case of flooding, the levee-building society always face a higher loss then the levee less society, which is expresses a the levee effect.

Therefore, it can be concluded in general that under climate projected water levels the levee effect varies under different climate scenarios. The levee effect is highest under the assumption of RCP 8.5 and non-stationary storm surges. Additionally, the uncertainties in the consideration of future developments are significantly higher for the levee-building society, especially under consideration of non-stationary storm surges.

Since no artificial data were used in this thesis to initialize the water level, as in Di Baldassarre et al. (2015), the assumptions about the levee effect are more objective. The model, adopted by Di Baldassarre et al. (2015), can withstand certain criticism, for example by model immanent human activities, but these are limited to a few behavioral drivers and decision making (Massuel et al. 2018). The differential equations reflect the logic described in the hypothesis of Di Baldassarre et al. (2015) (Massuel et al. 2018). Thus only patterns can be reproduced or observations made between the model variables.

[5] https://www.munichre.com/site/corporate/get/documents_E942261833/mr/assetpool.shared/Documents/0_Corporate_Website/6_Media_Relations/Press_Dossiers/50th_anniversary_storm_surge_hamburg/historical-storm-surge-events-en.pdf

A transdisciplinary approach and a stronger involvement of social science findings and observations in relation to human behavior would certainly be beneficial for the model and would allow deeper insights into humans individual behavior. The implication of SSPs provides an even more comprehensive perspective on future social developments. This broad approach aims to support decision-making by exploring possible ways of economic development and population growth. It takes into account societal decisions and actions that impact greenhouse gas emissions. Including this approach would lead to more meaningful projections in case of social developments.

With this work a research gap between flood risk management with integrated climate change scenarios and socio-hydrological modeling was narrowed. At the same time, however, there is still a great demand for better integration of human behavior and social development into model projections.

Acknowledgments
The model code is listed in the supplement. Selected parts of the code are published at https://github.com/scrim-network/BRICK.

I thank Prof. Dr. Tobias Krüger for his supervision, sharpening my focus and supporting me with critical questions and literature. I thank Jun.-Prof. Dr. Nicole Glanemann, for the topic finding, providing me with data and her supervision. Last but not least, I thank Robert Gieseke, Kilian Kuhla and Sven Willner for their constructive contributions around this thesis and all critical questions.

References

Bakker, A. M., Wong, T. E., Ruckert, K. L., & Keller, K. (2017). Sea-level projections representing the deeply uncertain contribution of the west antarctic ice sheet. *Scientific Reports*, *7*(1), 3880.

Baldassarre, G. D., Viglione, A., Carr, G., Kuil, L., Salinas, J., & Blöschl, G. (2013). Socio-hydrology: conceptualising human-flood interactions. *Hydrology and Earth System Sciences*, *17*(8), 3295–3303.

Barendrecht, M. H., Viglione, A., & Blöschl, G. (2017). A dynamic framework for flood risk. *Water Security*, *1*, 3–11.

Da Deppo, L., Datei, C., & Salandin, P. (2004). *Sistemazione dei corsi d'acqua*. Libreria Cortina.

Der Kiureghian, A., & Ditlevsen, O. (2009). Aleatory or epistemic? does it matter? *Structural Safety*, *31*(2), 105–112.

Di Baldassarre, G., Viglione, A., Carr, G., Kuil, L., Yan, K., Brandimarte, L., & Blöschl, G. (2015). Debates-perspectives on socio-hydrology: Capturing feedbacks between physical and social processes. *Water Resources Research*, *51*(6), 4770–4781.

Eijgenraam, C., Brekelmans, R., den Hertog, D., & Roos, K. (2012). Flood prevention by optimal dike heightening. *Delft University of Technology, the Netherlands Working Paper*.

Eijgenraam, C., Brekelmans, R., den Hertog, D., & Roos, K. (2016). Optimal strategies for flood prevention. *Management Science*, *63*(5), 1644–1656.

Eijgenraam, C. J. (2006). Optimal safety standards for dike-ring areas. *Discussion paper nr. 62, ISBN 90-5833-267-5*.

Garner, G. G., & Keller, K. (2018). Using direct policy search to identify robust strategies in adapting to uncertain sea-level rise and storm surge. *Environmental Modelling & Software*, *107*, 96–104.

Grames, J., Prskawetz, A., Grass, D., Viglione, A., & Blöschl, G. (2016). Modeling the interaction between flooding events and economic growth. *Ecological Economics*, *129*, 193–209.

Hall, J. W., Lempert, R. J., Keller, K., Hackbarth, A., Mijere, C., & McInerney, D. J. (2012).

Robust climate policies under uncertainty: a comparison of robust decision making and info-gap methods. *Risk Analysis: An International Journal*, *32*(10), 1657–1672.

Heine, R. A., & Pinter, N. (2012). Levee effects upon flood levels: an empirical assessment. *Hydrological Processes*, *26*(21), 3225–3240.

Hoffman, F. O., & Hammonds, J. S. (1994). Propagation of uncertainty in risk assessments: the need to distinguish between uncertainty due to lack of knowledge and uncertainty due to variability. *Risk analysis*, *14*(5), 707–712.

Jongman, B., Hochrainer-Stigler, S., Feyen, L., Aerts, J. C., Mechler, R., Botzen, W. W., ... Ward, P. J. (2014). Increasing stress on disaster-risk finance due to large floods. *Nature Climate Change*, *4*(4), 264.

Jongman, B., Ward, P. J., & Aerts, J. C. (2012). Global exposure to river and coastal flooding: Long term trends and changes. *Global Environmental Change*, *22*(4), 823–835.

Keller, K., & Srikrishnan, V. A. (2019, submitted). Ice sheet observations provide economic value of information for coastal flood risk management. *Risk Analysis*.

Kron, W. (2005). Flood risk= hazard - values - vulnerability. *Water International*, *30*(1), 58–68.

Lenton, T. M., Held, H., Kriegler, E., Hall, J. W., Lucht, W., Rahmstorf, S., & Schellnhuber, H. J. (2008). Tipping elements in the earth's climate system. *Proceedings of the national Academy of Sciences*, *105*(6), 1786–1793.

Martins, E. S., & Stedinger, J. R. (2000). Generalized maximum-likelihood generalized extreme-value quantile estimators for hydrologic data. *Water Resources Research*, *36*(3), 737–744.

Massuel, S., Riaux, J., Molle, F., Kuper, M., Ogilvie, A., Collard, A.-L., ... Barreteau, O. (2018). Inspiring a broader socio-hydrological negotiation approach with interdisciplinary field-based experience. *Water Resources Research*, *54*(4), 2510–2522.

Me-Bar, Y., & Valdez Jr, F. (2004). Recovery time after a disaster and the ancient maya. *Journal of Archaeological Science*, *31*(9), 1311–1324.

Muis, S., Güneralp, B., Jongman, B., Aerts, J. C., & Ward, P. J. (2015). Flood risk and adaptation strategies under climate change and urban expansion: A probabilistic analysis using global data. *Science of the Total Environment*, *538*, 445–457.

Munich Re. (2016). *Topics geo. natural catastrophes 2016: Analyses, assessments, positions. munich re group, munich.*

Oddo, P. C., Lee, B. S., Garner, G. G., Srikrishnan, V., Reed, P. M., Forest, C. E., & Keller, K. (2017). Deep uncertainties in sea-level rise and storm surge projections: Implications for coastal flood risk management. *Risk Analysis*.

ONeill, B. C., Kriegler, E., Riahi, K., Ebi, K. L., Hallegatte, S., Carter, T. R., ... van Vuuren, D. P. (2014). A new scenario framework for climate change research: the concept of shared socioeconomic pathways. *Climatic change*, *122*(3), 387–400.

Penning-Rowsell, E. C., et al. (2010). The benefits of flood and coastal risk management: a handbook of assessment techniques 2010.

Riahi, K., Van Vuuren, D. P., Kriegler, E., Edmonds, J., Oneill, B. C., Fujimori, S., ... others (2017). The shared socioeconomic pathways and their energy, land use, and greenhouse gas emissions implications: an overview. *Global Environmental Change*, *42*, 153–168.

Schaller, N., Kay, A. L., Lamb, R., Massey, N. R., Van Oldenborgh, G. J., Otto, F. E., ... others (2016). Human influence on climate in the 2014 southern england winter floods and their impacts. *Nature Climate Change*, *6*(6), 627.

Schönwiese, C.-D. (2013). *Praktische statistik für meteorologen und geowissenschaftler.* Stuttgart, Germany: Schweizerbart Science Publishers.

Scolobig, A., De Marchi, B., & Borga, M. (2012). The missing link between flood risk awareness and preparedness: findings from case studies in an alpine region. *Natural Hazards*, *63*(2), 499–520.

Stocker, T. (2014). *Climate change 2013: the physical science basis: Working group i contribution to the fifth assessment report of the intergovernmental panel on climate change.* Cambridge University Press.

Tanoue, M., Hirabayashi, Y., & Ikeuchi, H. (2016). Global-scale river flood vulnerability in the last 50 years. *Scientific reports*, *6*, 36021.

Van Dantzig, D. (1956). Economic decision problems for flood prevention. *Econometrica: Journal of the Econometric Society*, 276–287.

van Oldenborgh, G. J., Philip, S., Aalbers, E., Vautard, R., Otto, F., Haustein, K., ... Cullen, H. (2016). Rapid attribution of the may/june 2016 flood-inducing precipitation in france and germany to climate change. *Hydrol Earth Syst Sci Discuss doi*, *10*.

Viglione, A., Di Baldassarre, G., Brandimarte, L., Kuil, L., Carr, G., Salinas, J. L., ... Blöschl, G. (2014). Insights from socio-hydrology modelling on dealing with flood risk–roles of collective memory, risk-taking attitude and trust. *Journal of Hydrology*, *518*, 71–82.

Warmink, J. J., Janssen, J., Booij, M. J., & Krol, M. S. (2010). Identification and classification of uncertainties in the application of environmental models. *Environmental modelling & software*, *25*(12), 1518–1527.

Wesselink, A., Kooy, M., & Warner, J. (2017). Socio-hydrology and hydrosocial analysis: toward dialogues across disciplines. *Wiley Interdisciplinary Reviews: Water*, *4*(2), e1196.

Westerberg, I. K., Di Baldassarre, G., Beven, K. J., Coxon, G., & Krueger, T. (2017). Perceptual models of uncertainty for socio-hydrological systems: a flood risk change example. *Hydrological sciences journal*, *62*(11), 1705–1713.

Willner, S. N., Levermann, A., Zhao, F., & Frieler, K. (2018). Adaptation required to preserve future high-end river flood risk at present levels. *Science advances*, *4*(1), eaao1914.

Winsemius, H. C., Aerts, J. C., van Beek, L. P., Bierkens, M. F., Bouwman, A., Jongman, B., ... others (2016). Global drivers of future river flood risk. *Nature Climate Change*, *6*(4), 381.

Wong, T. E., Bakker, A. M., Ruckert, K., Applegate, P., Slangen, A., & Keller, K. (2017). Brick v0. 2, a simple, accessible, and transparent model framework for climate and regional sea-level projections. *Geoscientific Model Development*, *10*(7), 2741–2760.

Zeeberg, J. (2009). *Flood control in the netherlands.* `https://www.rijnland.net/downloads/floodcontrolrijnland-1-1.pdf` (accessed Marche 14, 2019). Hoogheemraadschap van Rijnland.

6 Supplement

Table 1: Parameters and Values. Time invariant parameters of the dynamic model and used values with references following Di Baldassarre et al. (2015).

	Dimension	Description	Values and References
α_H	[L]	Parameter related to relationship between flood water levels to relative damage	10 m Penning-Rowsell et al. (2010)
ξ_H		Proportion of flood level enhancement due to presence of levees	0.2 Heine and Pinter (2012)
ρ_D	[T^{-1}]	Maximum relative growth rate	0.03 $year^{-1}$ Me-Bar and Valdez Jr (2004)
α_D		Ratio preparedness/awareness	5 Scolobig, De Marchi, and Borga (2012)
ε_T		Safety factor for levee heightening	1.1 Da Deppo, Datei, and Salandin (2004)
κ_T	[T^{-1}]	Protection level decay rate	$2 \cdot 10^{-05}$ $year^{-1}$ Baldassarre et al. (2013)
μ_s	[T^{-1}]	Memory loss rate	0.06 $year^{-1}$ Baldassarre et al. (2013)

Table 2: Initial values. Time varying variables of the dynamic model and initial conditions following Di Baldassarre et al. (2015).

	Dimension	Description	Initial values
F		Relative flood damage	1.0
H	[L]	Height of levees	0
D		Population density	0.1
M		Societal memory of floods	0

Table 3: Annual median value of water levels.

RCP	year	stationary storm surges	non-stationary storm surges
2.6	2017	3.10 m	3.10 m
	2100	3.40 m	3.60 m
4.5	2017	3.10 m	3.10 m
	2100	3.50 m	4.14 m
6.0	2017	3.10 m	3.04 m
	2100	3.50 m	4.50 m
8.5	2017	3.10 m	3.10 m
	2100	3.90 m	5.60 m

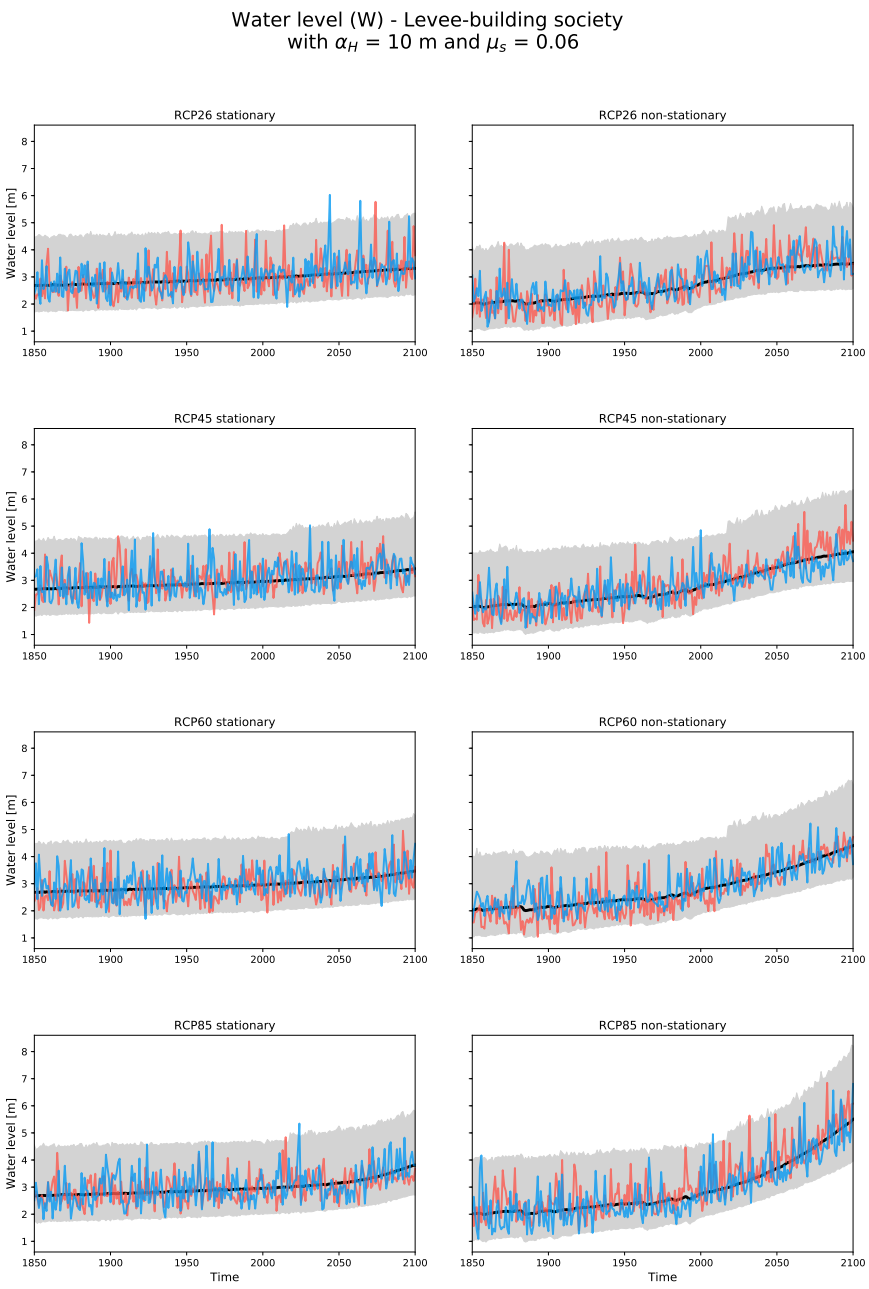

Figure 6: Initial water level for the levee-building society. The variable water level for the RCP scenario 2.6, 4.5, 6.0 and 8.5, under consideration of stationarity (left) and non-stationary (right) storm surges are depicted. For the expected maximum and minimum values of the distribution, the 99.5% quantile and the 0.5% quantile were regarded as upper and lower limits. The range of both quantiles can be seen in the gray bars in this figure. The black lines show the median of the projected distributions. The red and blue lines correspond to two different time series of the projected data and illustrate how the time series are shaped. Here, a temporal resolution with annual time steps from 2017 to 2100 is shown. Here, a temporal resolution with annual time steps from 1850 to 2100 is shown.

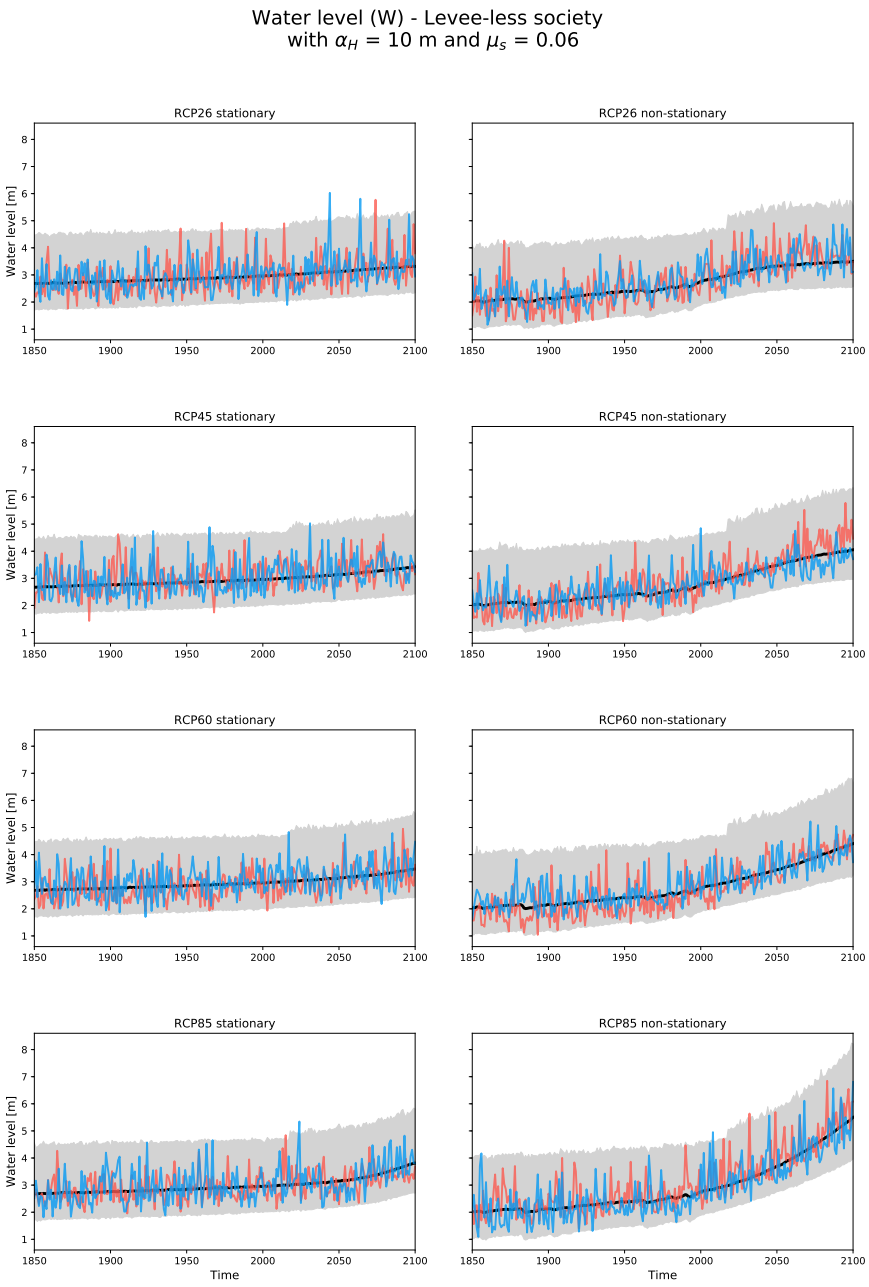

Figure 7: Initial water level for the levee-less society. The variable water level for the RCP scenario 2.6, 4.5, 6.0 and 8.5, under consideration of stationarity (left) and non-stationary (right) storm surges are depicted. For the expected maximum and minimum values of the distribution, the 99.5% quantile and the 0.5% quantile were regarded as upper and lower limits. The range of both quantiles can be seen in the gray bars in this figure. The black lines show the median of the projected distributions. The red and blue lines correspond to two different time series of the projected data and illustrate how the time series are shaped. Here, a temporal resolution with annual time steps from 2017 to 2100 is shown. Here, a temporal resolution with annual time steps from 1850 to 2100 is shown.

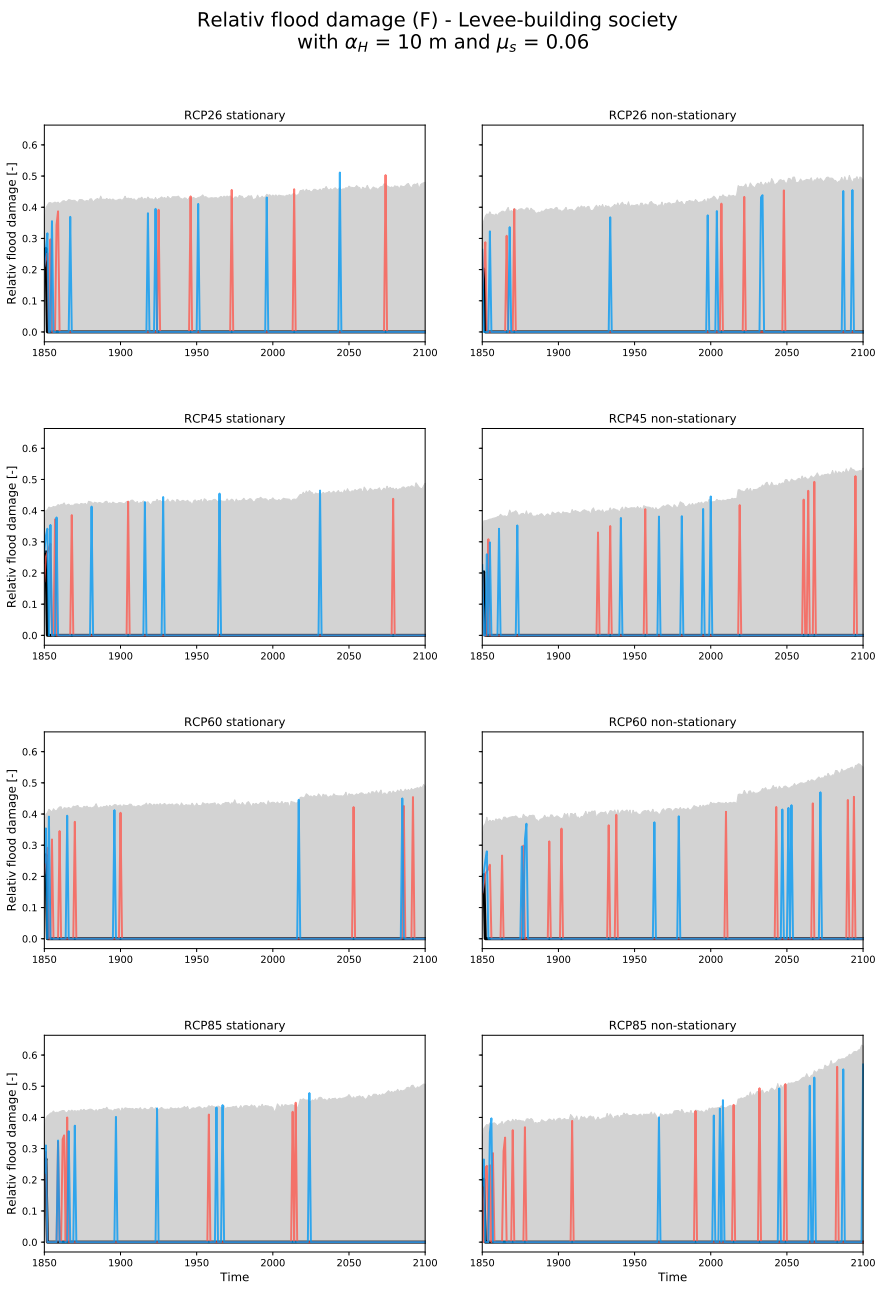

Figure 8: The flood damage for the levee-building society. The variable flood damage for the RCP scenario 2.6, 4.5, 6.0 and 8.5, under consideration of stationarity (left) and non-stationary (right) storm surges are depicted. For the expected maximum and minimum values of the distribution, the 99.5% quantile and the 0.5% quantile were regarded as upper and lower limits. The range of both quantiles can be seen in the gray bars in this figure. The black lines show the median of the projected distributions. The red and blue lines correspond to two different time series of the projected data and illustrate how the time series are shaped. Here, a temporal resolution with annual time steps from 2017 to 2100 is shown. Here, a temporal resolution with annual time steps from 1850 to 2100 is shown.

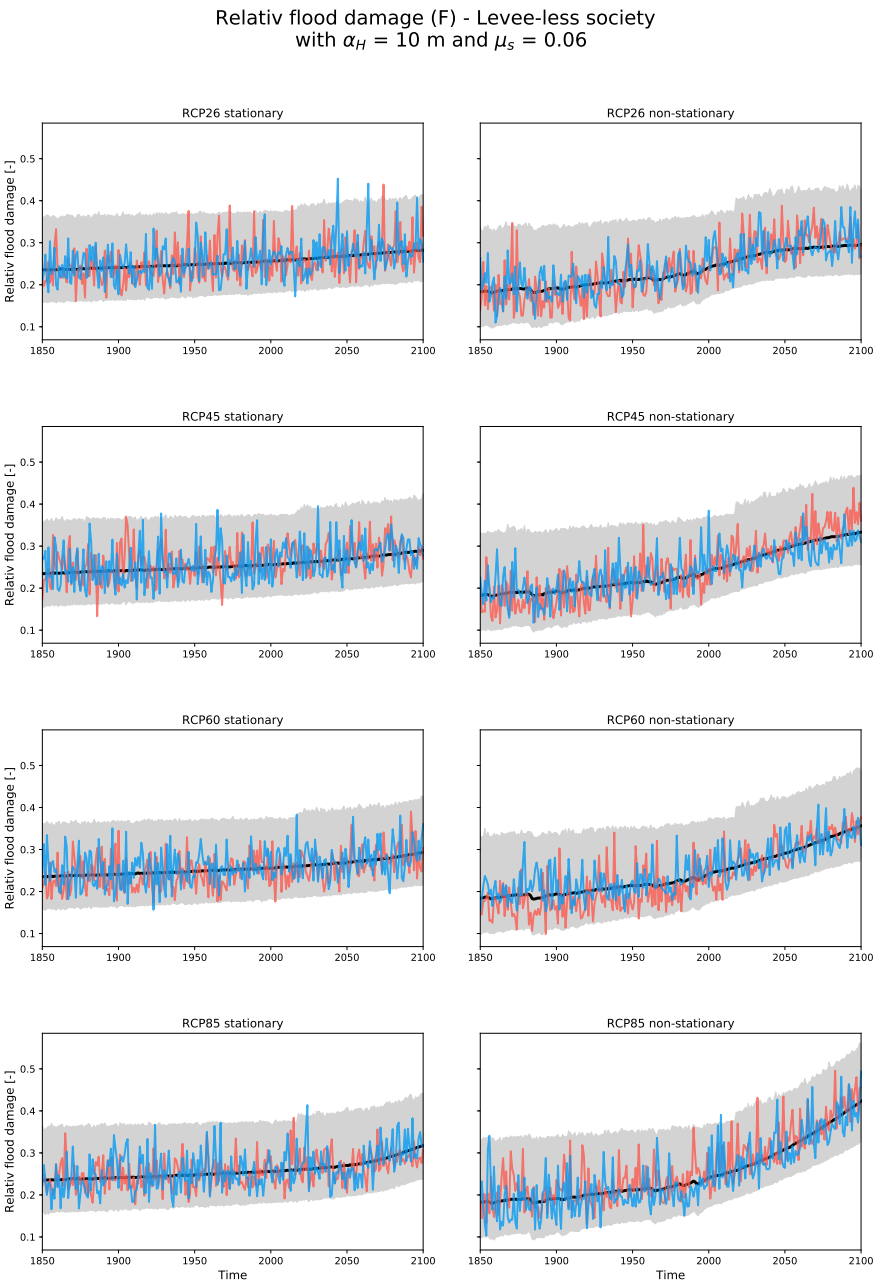

Figure 9: The flood damage for the levee-less society. The variable flood damage for the RCP scenario 2.6, 4.5, 6.0 and 8.5, under consideration of stationarity (left) and non-stationary (right) storm surges are depicted. For the expected maximum and minimum values of the distribution, the 99.5% quantile and the 0.5% quantile were regarded as upper and lower limits. The range of both quantiles can be seen in the gray bars in this figure. The black lines show the median of the projected distributions. The red and blue lines correspond to two different time series of the projected data and illustrate how the time series are shaped. Here, a temporal resolution with annual time steps from 2017 to 2100 is shown. Here, a temporal resolution with annual time steps from 1850 to 2100 is shown.

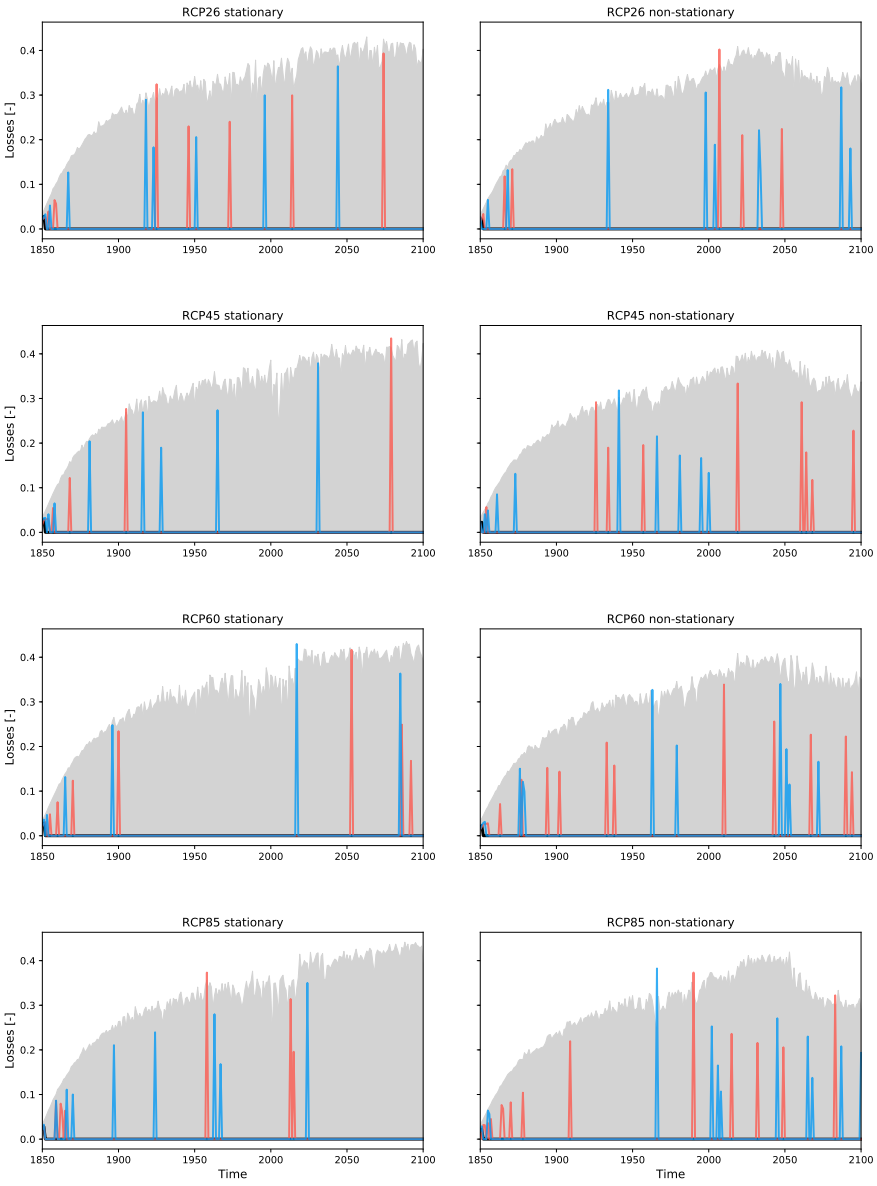

Figure 10: Loss for the levee-building society. The variable loss for the RCP scenario 2.6, 4.5, 6.0 and 8.5, under consideration of stationarity (left) and non-stationary (right) storm surges are depicted. For the expected maximum and minimum values of the distribution, the 99.5% quantile and the 0.5% quantile were regarded as upper and lower limits. The range of both quantiles can be seen in the gray bars in this figure. The black lines show the median of the projected distributions. The red and blue lines correspond to two different time series of the projected data and illustrate how the time series are shaped. Here, a temporal resolution with annual time steps from 2017 to 2100 is shown. Here, a temporal resolution with annual time steps from 1850 to 2100 is shown.

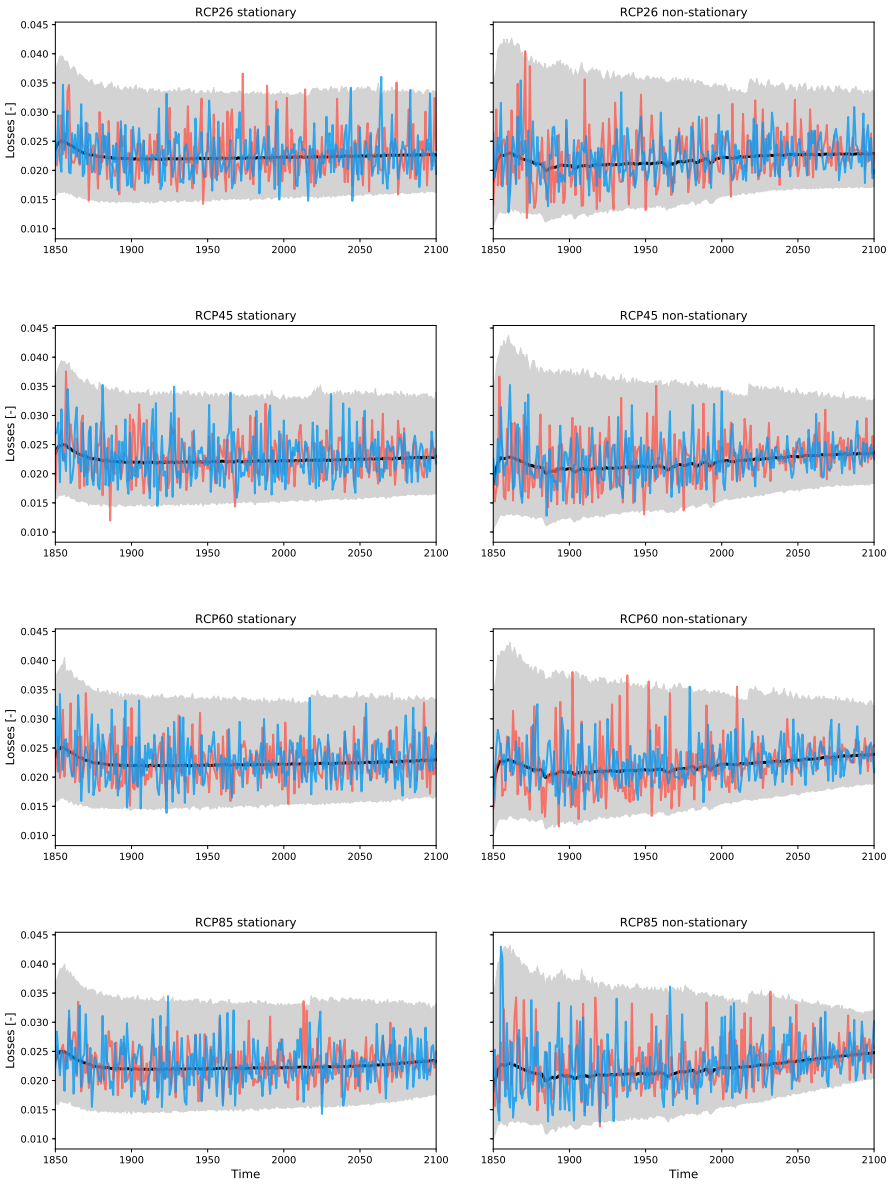

Figure 11: Loss for the levee-less society. The variable loss for the RCP scenario 2.6, 4.5, 6.0 and 8.5, under consideration of stationarity (left) and non-stationary (right) storm surges are depicted. For the expected maximum and minimum values of the distribution, the 99.5% quantile and the 0.5% quantile were regarded as upper and lower limits. The range of both quantiles can be seen in the gray bars in this figure. The black lines show the median of the projected distributions. The red and blue lines correspond to two different time series of the projected data and illustrate how the time series are shaped. Here, a temporal resolution with annual time steps from 2017 to 2100 is shown. Here, a temporal resolution with annual time steps from 1850 to 2100 is shown.

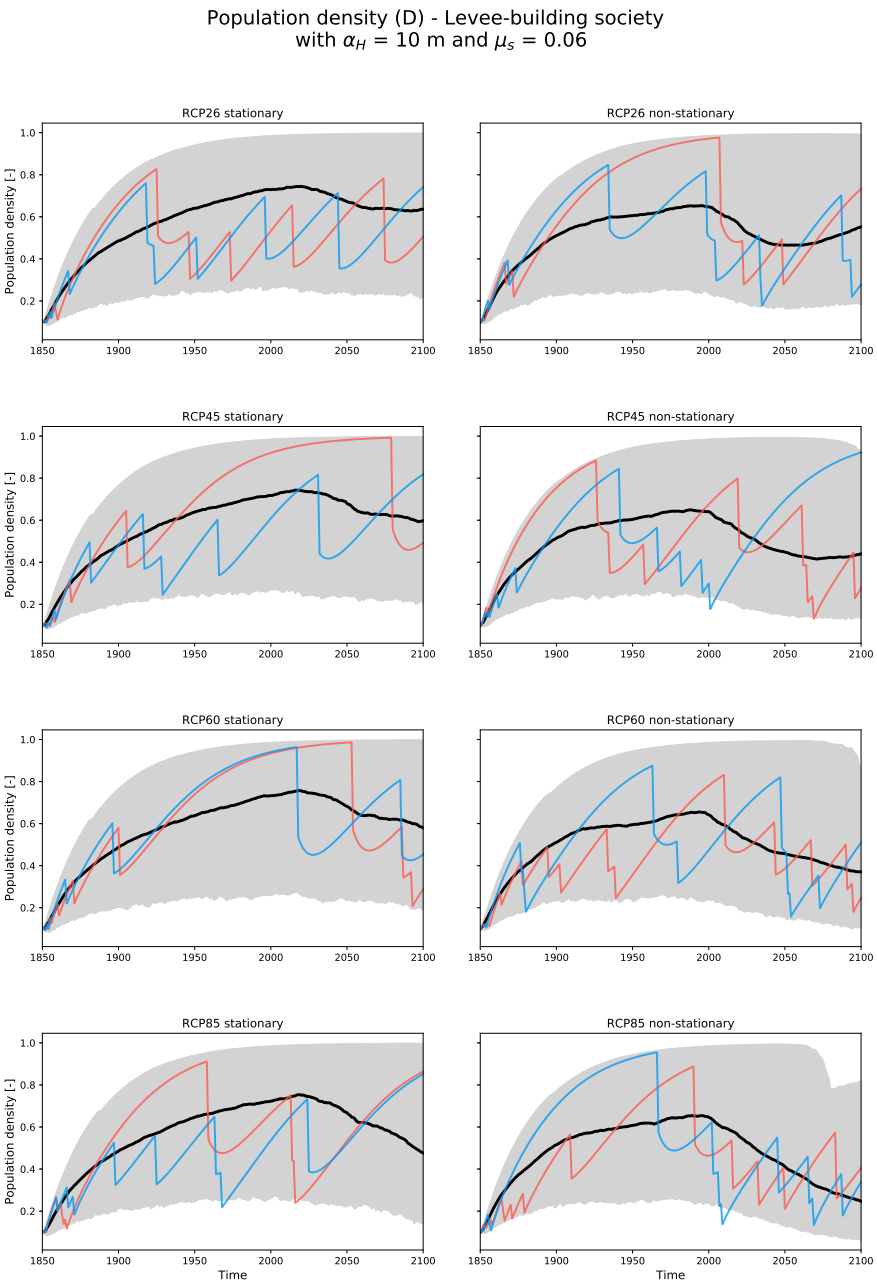

Figure 12: Population density for the levee-building society. The variable population density for the RCP scenario 2.6, 4.5, 6.0 and 8.5, under consideration of stationarity (left) and non-stationary (right) storm surges are depicted. For the expected maximum and minimum values of the distribution, the 99.5% quantile and the 0.5% quantile were regarded as upper and lower limits. The range of both quantiles can be seen in the gray bars in this figure. The black lines show the median of the projected distributions. The red and blue lines correspond to two different time series of the projected data and illustrate how the time series are shaped. Here, a temporal resolution with annual time steps from 2017 to 2100 is shown. Here, a temporal resolution with annual time steps from 1850 to 2100 is shown.

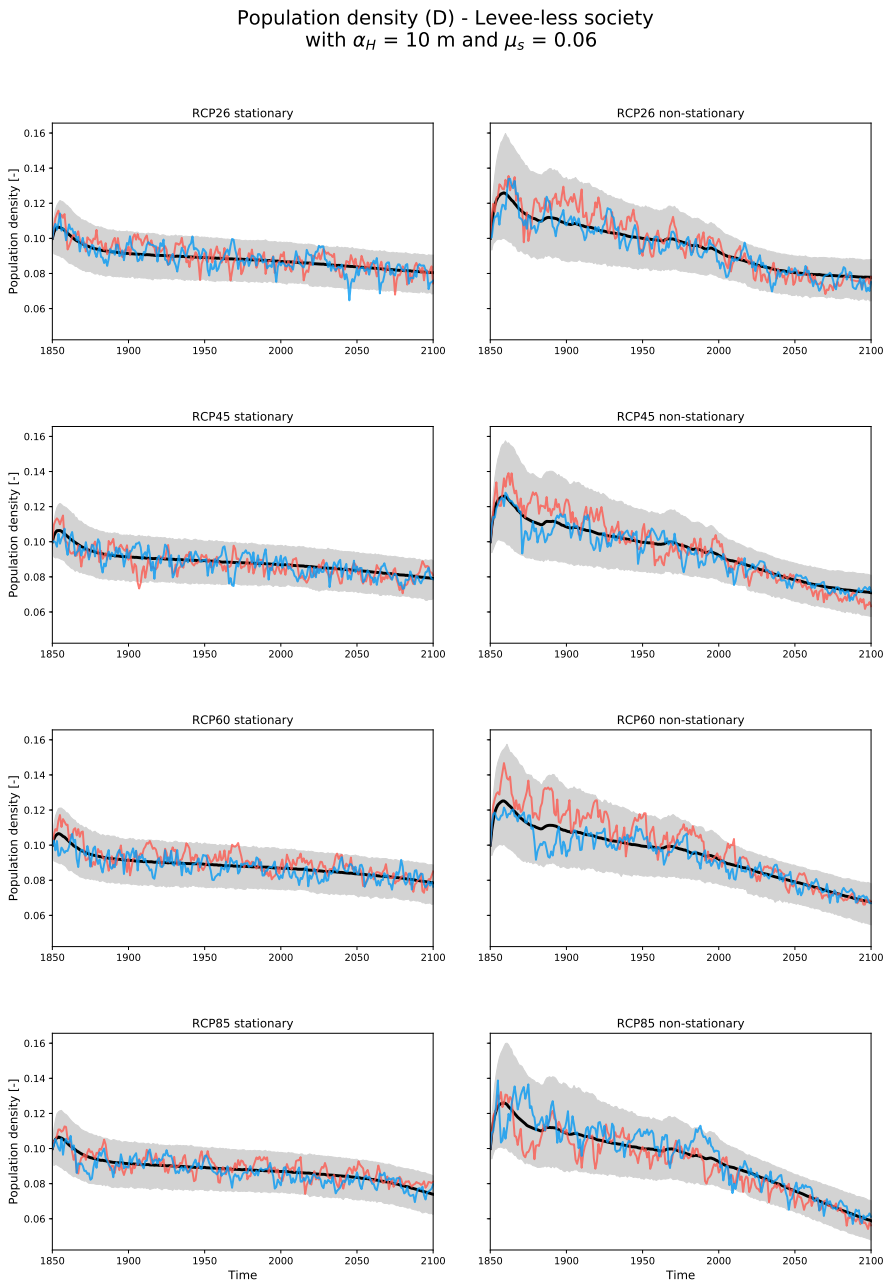

Figure 13: Population density for the levee-less society. The variable population density for the RCP scenario 2.6, 4.5, 6.0 and 8.5, under consideration of stationarity (left) and non-stationary (right) storm surges are depicted. For the expected maximum and minimum values of the distribution, the 99.5% quantile and the 0.5% quantile were regarded as upper and lower limits. The range of both quantiles can be seen in the gray bars in this figure. The black lines show the median of the projected distributions. The red and blue lines correspond to two different time series of the projected data and illustrate how the time series are shaped. Here, a temporal resolution with annual time steps from 2017 to 2100 is shown. Here, a temporal resolution with annual time steps from 1850 to 2100 is shown.

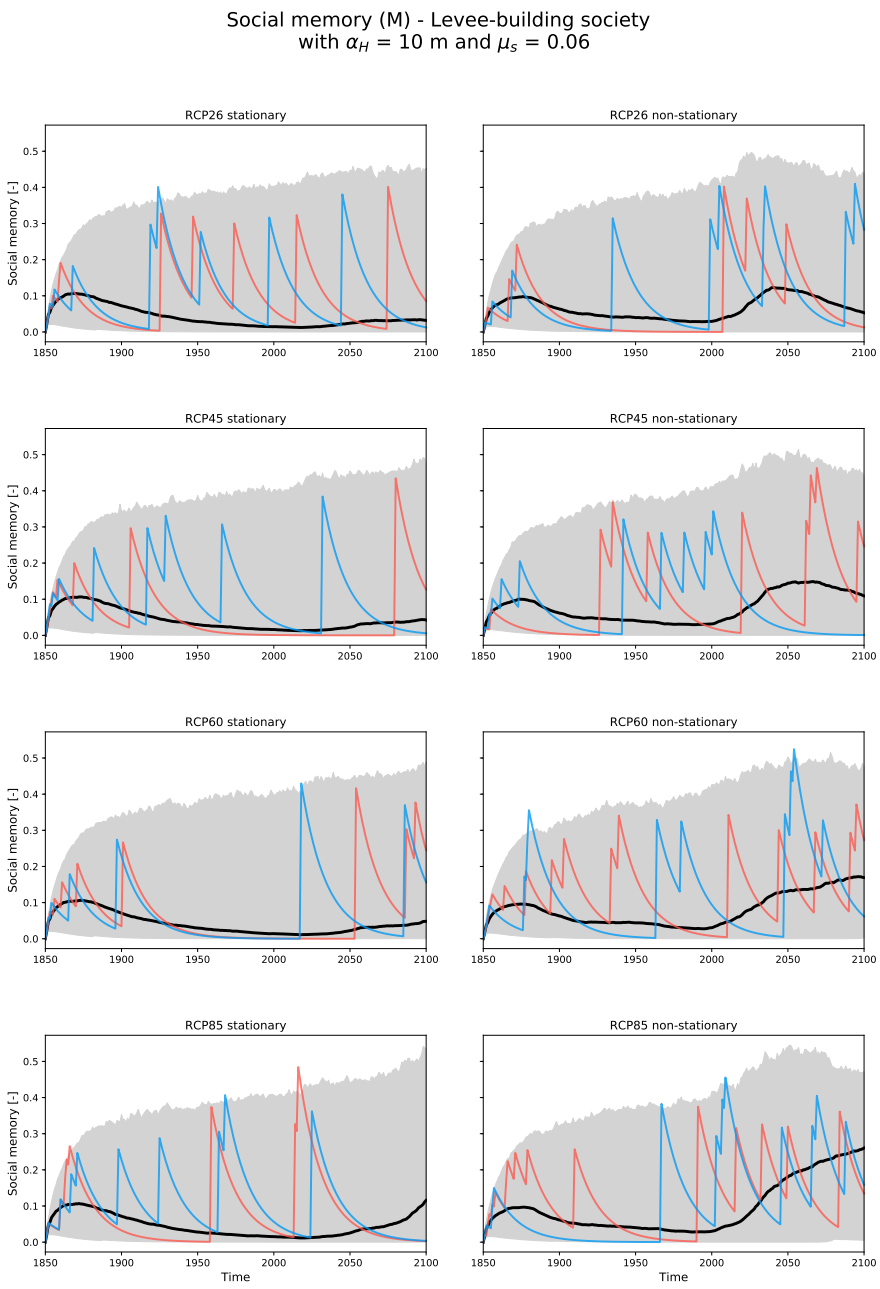

Figure 14: Social memory for the levee-building society. The variable social memory for the RCP scenario 2.6, 4.5, 6.0 and 8.5, under consideration of stationarity (left) and non-stationary (right) storm surges are depicted. For the expected maximum and minimum values of the distribution, the 99.5% quantile and the 0.5% quantile were regarded as upper and lower limits. The range of both quantiles can be seen in the gray bars in this figure. The black lines show the median of the projected distributions. The red and blue lines correspond to two different time series of the projected data and illustrate how the time series are shaped. Here, a temporal resolution with annual time steps from 2017 to 2100 is shown. Here, a temporal resolution with annual time steps from 1850 to 2100 is shown.

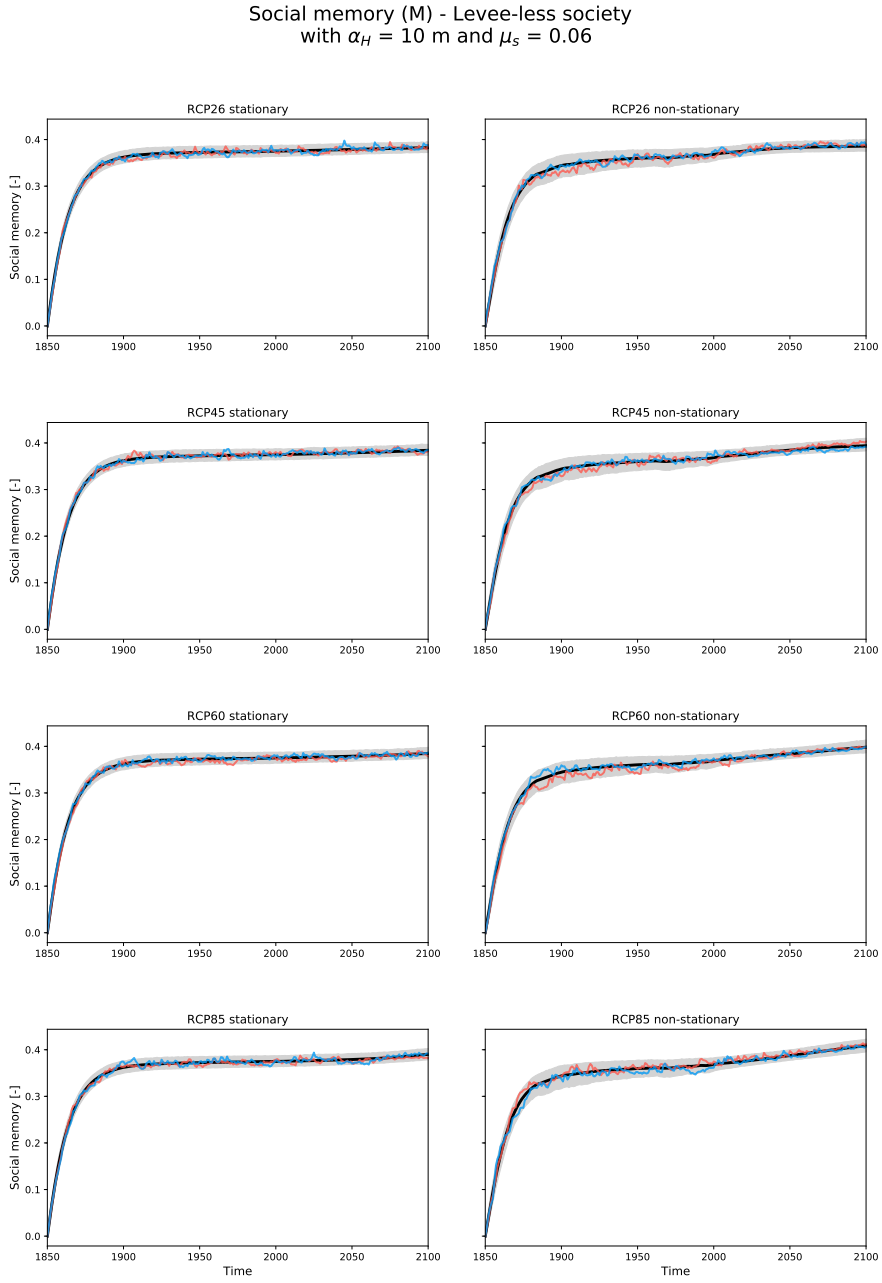

Figure 15: Social memory for the levee-less society. The variable social memory for the RCP scenario 2.6, 4.5, 6.0 and 8.5, under consideration of stationarity (left) and non-stationary (right) storm surges are depicted. For the expected maximum and minimum values of the distribution, the 99.5% quantile and the 0.5% quantile were regarded as upper and lower limits. The range of both quantiles can be seen in the gray bars in this figure. The black lines show the median of the projected distributions. The red and blue lines correspond to two different time series of the projected data and illustrate how the time series are shaped. Here, a temporal resolution with annual time steps from 2017 to 2100 is shown. Here, a temporal resolution with annual time steps from 1850 to 2100 is shown.

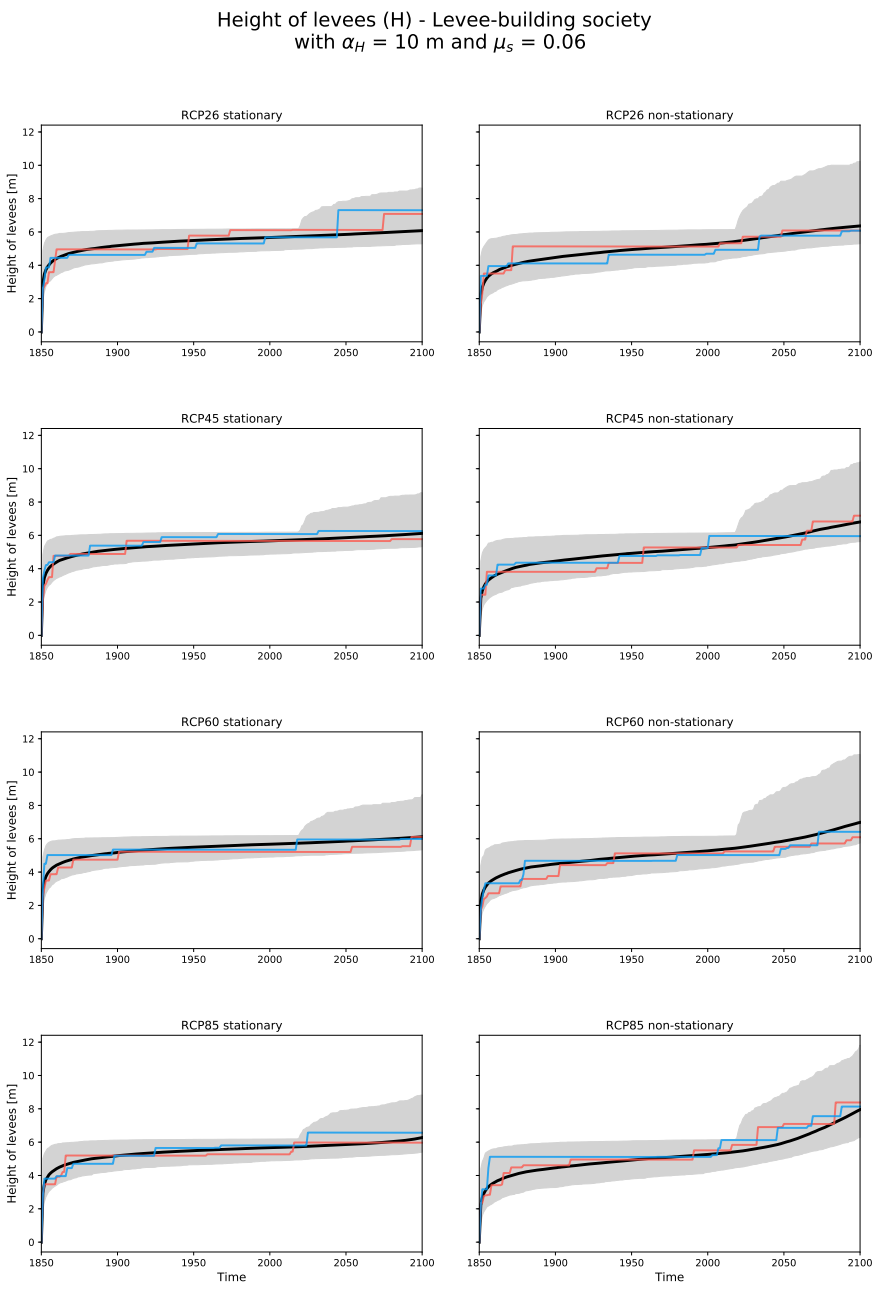

Figure 16: Levee height for the levee-building society. The variable levee height for the RCP scenario 2.6, 4.5, 6.0 and 8.5, under consideration of stationarity (left) and non-stationary (right) storm surges are depicted. For the expected maximum and minimum values of the distribution, the 99.5% quantile and the 0.5% quantile were regarded as upper and lower limits. The range of both quantiles can be seen in the gray bars in this figure. The black lines show the median of the projected distributions. The red and blue lines correspond to two different time series of the projected data and illustrate how the time series are shaped. Here, a temporal resolution with annual time steps from 2017 to 2100 is shown. Here, a temporal resolution with annual time steps from 1850 to 2100 is shown.

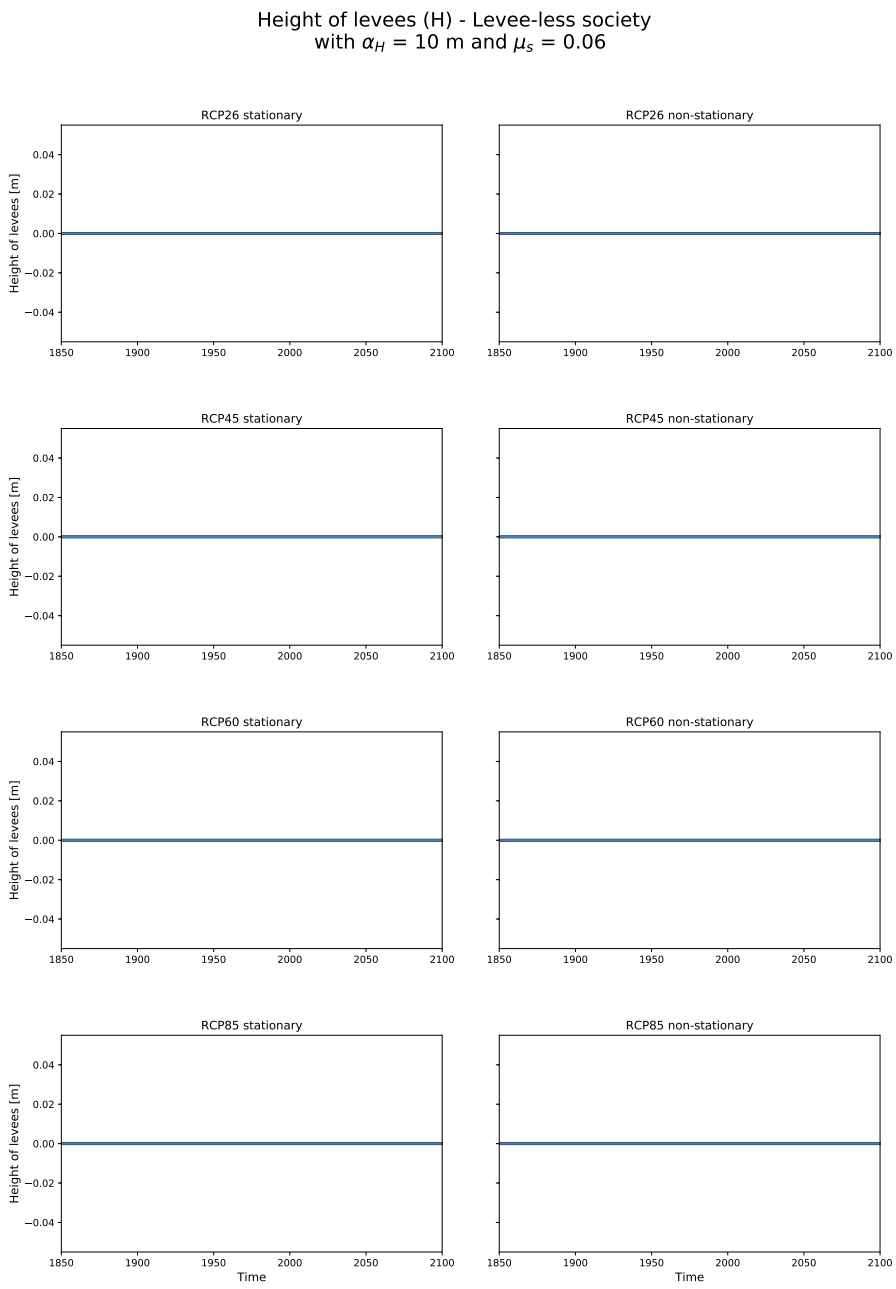

Figure 17: Levee height for the levee-less society. The variable levee height for the RCP scenario 2.6, 4.5, 6.0 and 8.5, under consideration of stationarity (left) and non-stationary (right) storm surges are depicted. For the expected maximum and minimum values of the distribution, the 99.5% quantile and the 0.5% quantile were regarded as upper and lower limits. The range of both quantiles can be seen in the gray bars in this figure. The black lines show the median of the projected distributions. The red and blue lines correspond to two different time series of the projected data and illustrate how the time series are shaped. Here, a temporal resolution with annual time steps from 2017 to 2100 is shown. Here, a temporal resolution with annual time steps from 1850 to 2100 is shown.

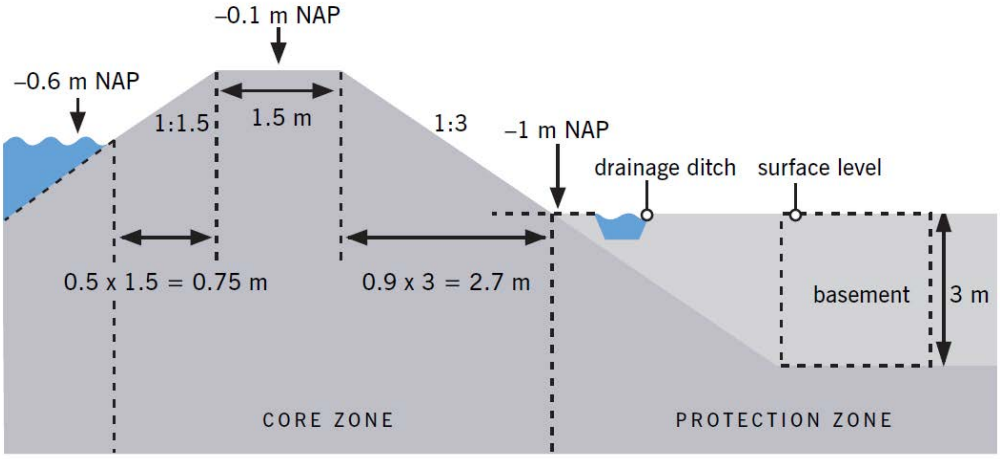

Figure 18: This profile shows that a levee about 2 m above the NAP requires a core zone of 5 m. In addition, a protection zone of 15 m on both sides of the core zone is required to ensure that a stable earth body remains next to the levee during excavation (Zeeberg 2009)

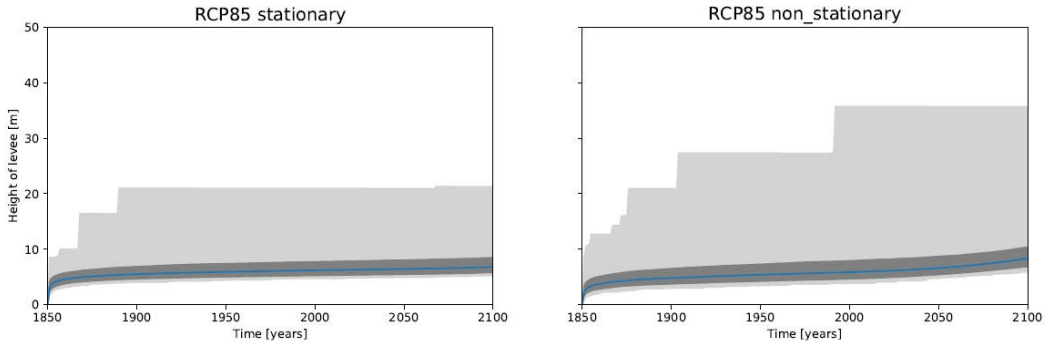

Figure 19: In a first model run, the water level was not adjusted for the time period between 1850 and 2017. The figure shows the projected heights of levees for RCP scenario 8.5 under the assumption of the tow different storm surge stationaryities. As a result, under consideration of non stationary of storm surges the levees should have been more than 15 m high before 1900.

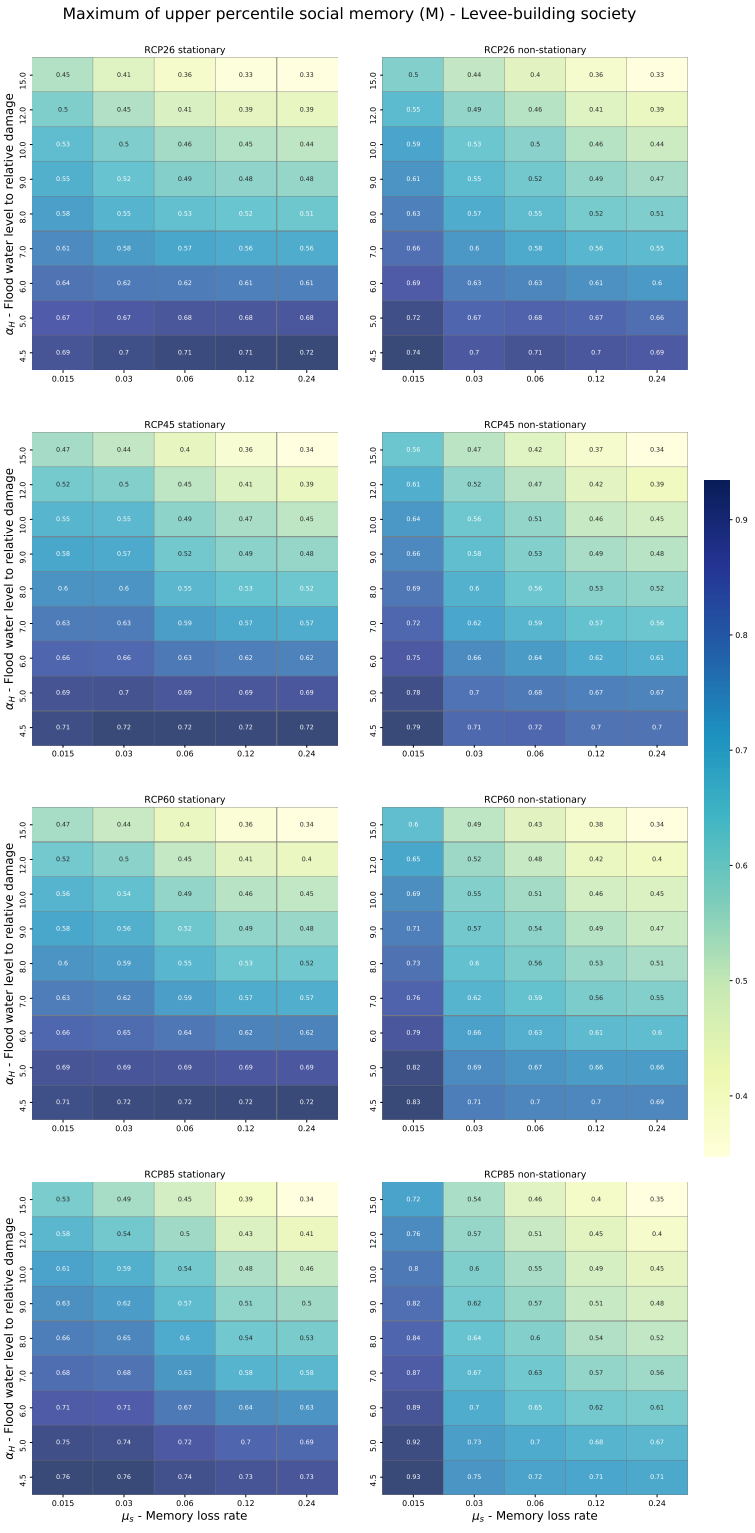

Figure 20: Heatmap - social memory for the levee-building society. The parameter analysis show the influence of the parameters floodwater vulnerability (α_H) and memory loss rate (μ_s) on the variable social memory, for the RCP scenarios 2.6, 4.5, 6.0 and 8.5, under consideration of stationarity (left) and non-stationary (right) storm surges. This analyses is using the maximum value of the 99.5%-quantile of the distribution of output variable.

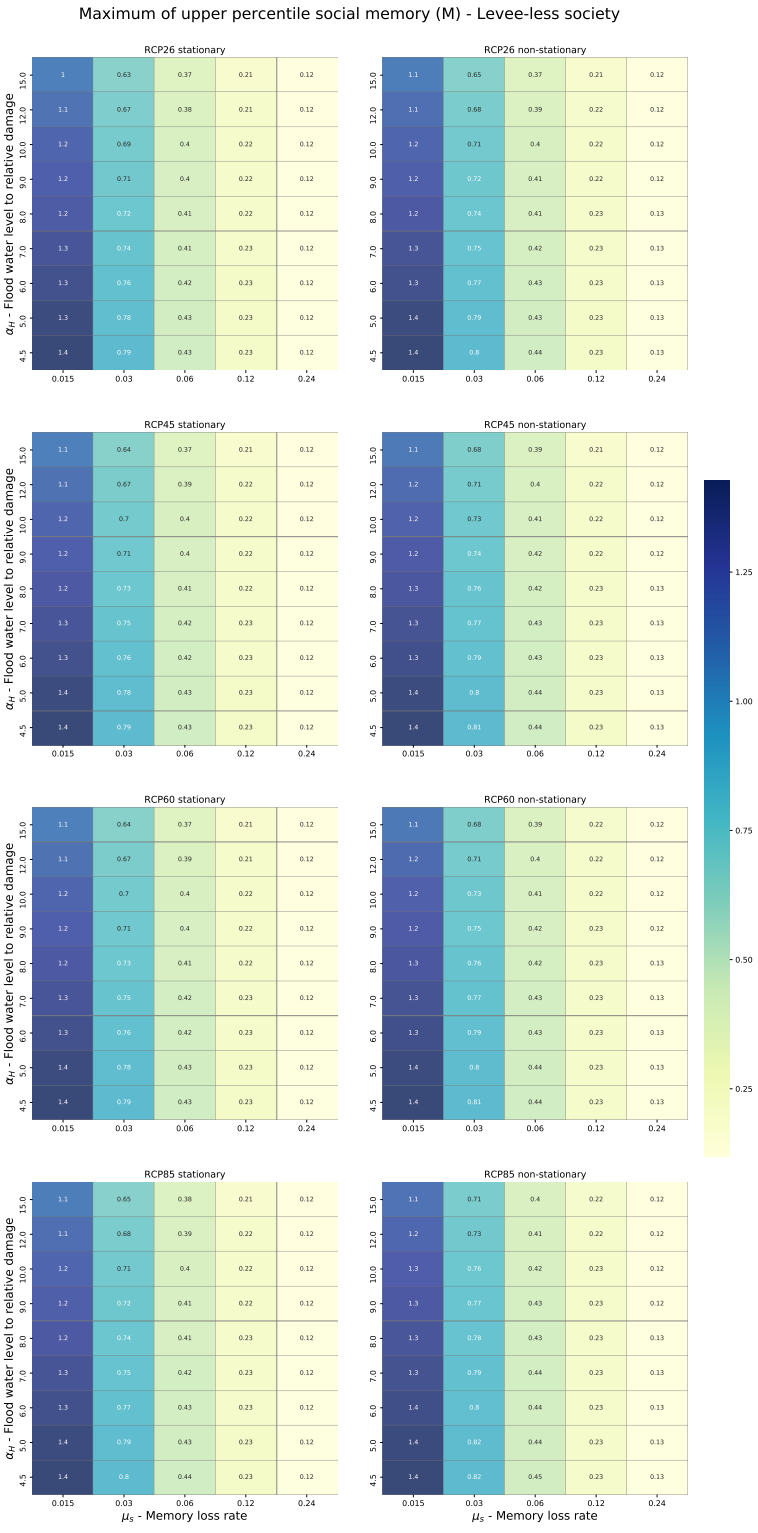

Figure 21: Heatmap - social memory for the levee-less society. The parameter analysis show the influence of the parameters floodwater vulnerability (α_H) and memory loss rate (μ_s) on the variable social memory, for the RCP scenarios 2.6, 4.5, 6.0 and 8.5, under consideration of stationarity (left) and non-stationary (right) storm surges. This analyses is using the maximum value of the 99.5%-quantile of the distribution of output variable.

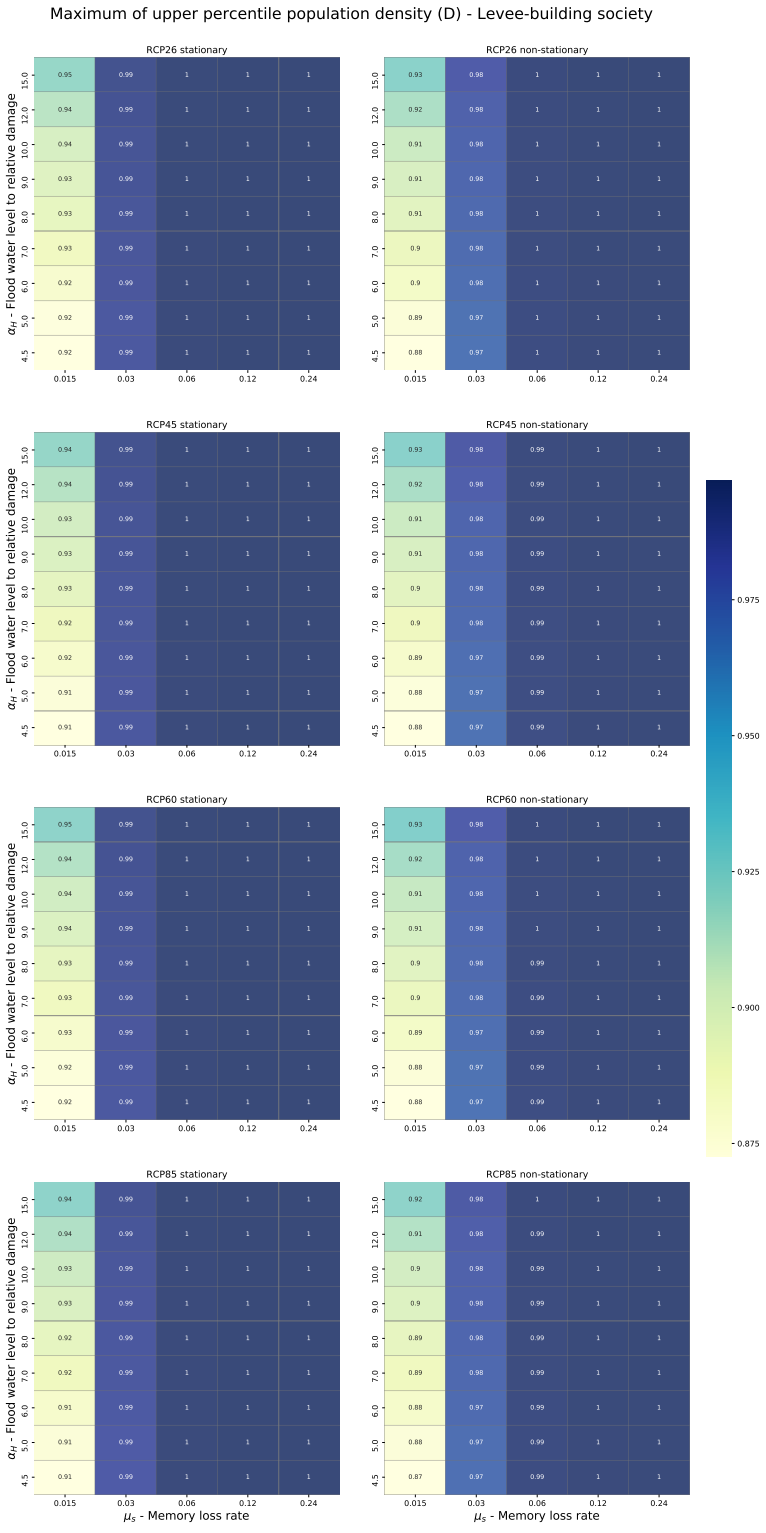

Figure 22: Heatmap - population density for the levee-building society. The parameter analysis show the influence of the parameters floodwater vulnerability (α_H) and memory loss rate (μ_s) on the variable population density, for the RCP scenarios 2.6, 4.5, 6.0 and 8.5, under consideration of stationarity (left) and non-stationary (right) storm surges. This analyses is using the maximum value of the 99.5%-quantile of the distribution of output variable.

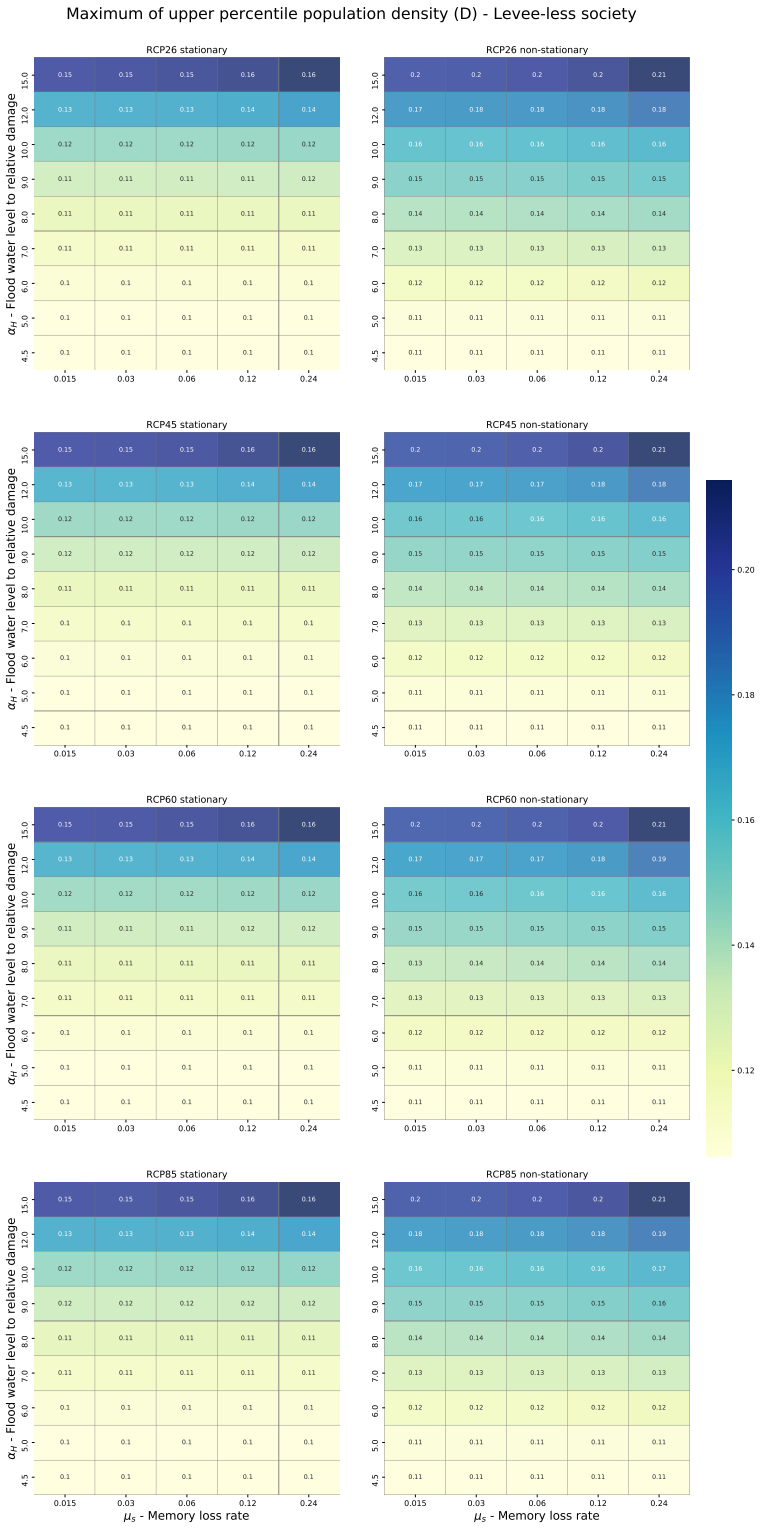

Figure 23: Heatmap - population density for the levee-less society. The parameter analysis show the influence of the parameters floodwater vulnerability (α_H) and memory loss rate (μ_s) on the variable population density, for the RCP scenarios 2.6, 4.5, 6.0 and 8.5, under consideration of stationarity (left) and non-stationary (right) storm surges. This analyses is using the maximum value of the 99.5%-quantile of the distribution of output variable.

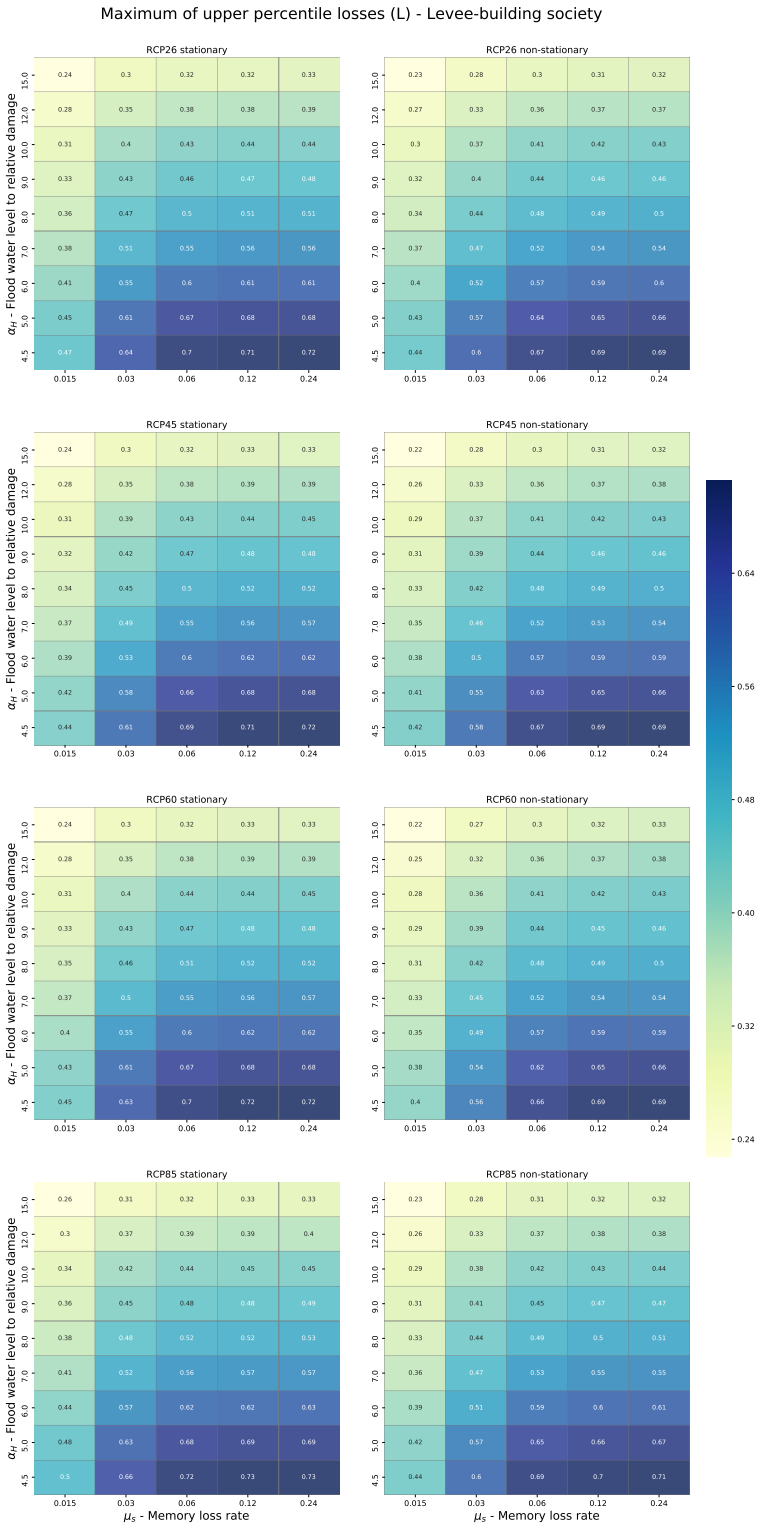

Figure 24: Heatmap - loss for the levee-building society. The parameter analysis show the influence of the parameters floodwater vulnerability (α_H) and memory loss rate (μ_s) on the variable loss, for the RCP scenarios 2.6, 4.5, 6.0 and 8.5, under consideration of stationarity (left) and non-stationary (right) storm surges. This analyses is using the maximum value of the 99.5%-quantile of the distribution of output variable.

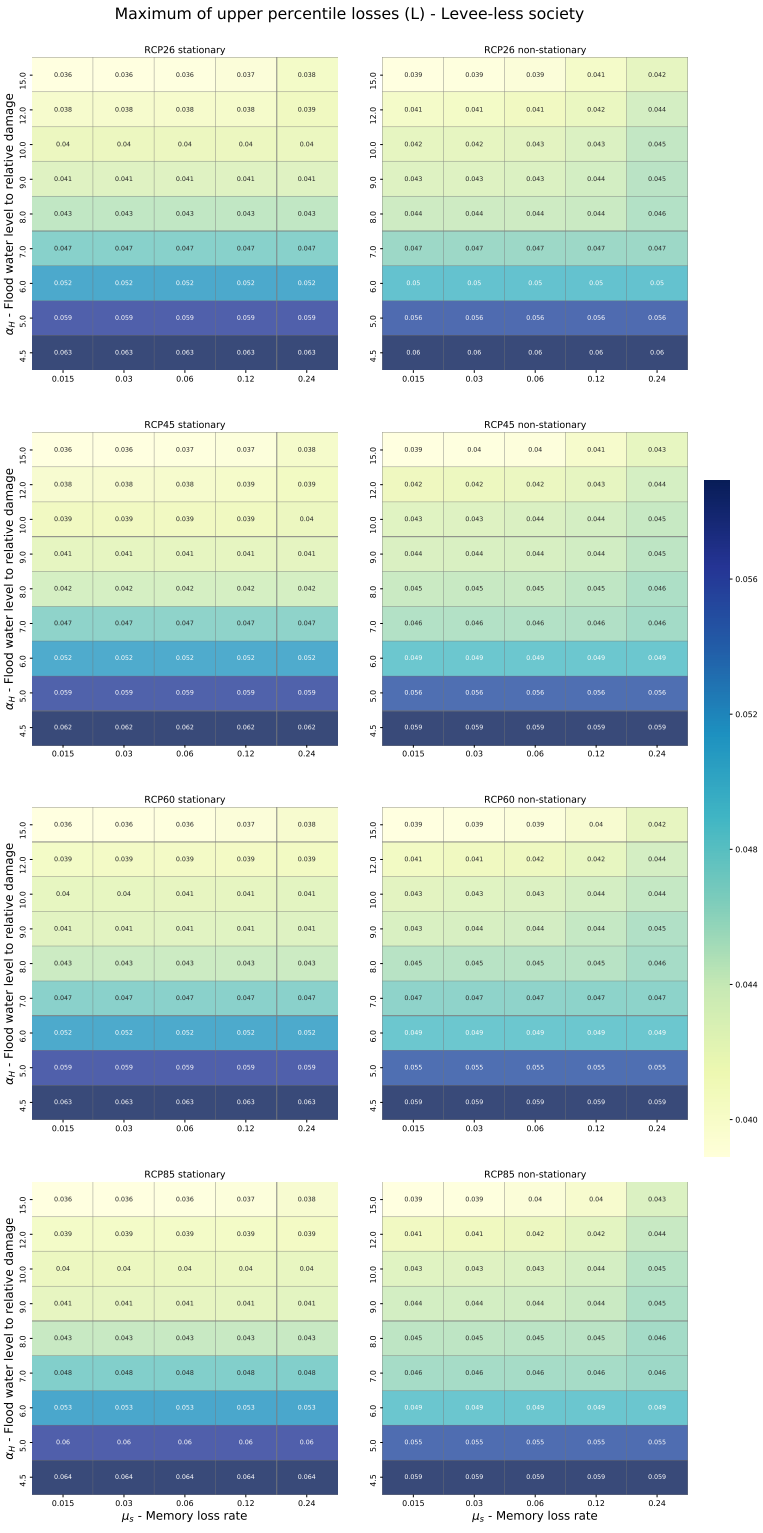

Figure 25: Heatmap - loss for the levee-less society. The parameter analysis show the influence of the parameters floodwater vulnerability (α_H) and memory loss rate (μ_s) on the variable loss, for the RCP scenarios 2.6, 4.5, 6.0 and 8.5, under consideration of stationarity (left) and non-stationary (right) storm surges. This analyses is using the maximum value of the 99.5%-quantile of the distribution of output variable.

ERKLÄRUNG

Ich erkläre, dass ich die vorliegende Arbeit nicht für andere Prüfungen eingereicht, selbständig und nur unter Verwendung der angegebenen Literatur und Hilfsmittel angefertigt habe. Sämtliche fremde Quellen inklusive Internetquellen, Grafiken, Tabellen und Bilder, die ich unverändert oder abgewandelt wiedergegeben habe, habe ich als solche kenntlich gemacht. Mir ist bekannt, dass Verstöße gegen diese Grundsätze als Täuschungsversuch bzw. Täuschung geahndet werden.

Berlin, den 18.04.2019

Unterschrift